Journal of Medicinal Chemistry

Article

pubs.acs.org/jmc

Combining Galantamine and Memantine in Multitargeted, New Chemical Entities Potentially Useful in Alzheimer's Disease

Elena Simoni,[†,‡] Simona Daniele,[†,§] Giovanni Bottegoni,[†] Daniela Pizzirani,[†] Maria L. Trincavelli,[§] Luca Goldoni,[†] Glauco Tarozzo,[†] Angelo Reggiani,[†] Claudia Martini,[§] Daniele Piomelli,[†,⊥] Carlo Melchiorre,[‡] Michela Rosini,*[,‡] and Andrea Cavalli*[,†,‡]

[†]Drug Discovery and Development, Istituto Italiano di Tecnologia, via Morego 30, 16163 Genova, Italy

[‡]Department of Pharmaceutical Sciences, Alma Mater Studiorum − Bologna University, via Belmeloro 6, 40126 Bologna, Italy

[§]Department of Psychiatry, Neurobiology, Pharmacology and Biotechnology, University of Pisa, via Bonanno 6, 56126 Pisa, Italy

[⊥]Departments of Pharmacology and Biological Chemistry, University of California, Irvine 92697-4621, United States

Supporting Information

ABSTRACT: Herein we report on a novel series of multitargeted compounds obtained by linking together galantamine and memantine. The compounds were designed by taking advantage of the crystal structures of acetylcholinesterase (AChE) in complex with galantamine derivatives. Sixteen novel derivatives were synthesized, using spacers of different lengths and chemical composition. The molecules were then tested as inhibitors of AChE and as binders of the *N*-methyl-D-aspartate (NMDA) receptor (NMDAR). Some of the new compounds were nanomolar inhibitors of AChE and showed micromolar affinities for NMDAR. All compounds were also tested for selectivity toward NMDAR containing the 2B subunit (NR2B). Some of the new derivatives showed a micromolar affinity for NR2B. Finally, selected compounds were tested using a cell-based assay to measure their neuroprotective activity. Three of them showed a remarkable neuroprotective profile, inhibiting the NMDA-induced neurotoxicity at subnanomolar concentrations (e.g., **5**, named memagal, IC_{50} = 0.28 nM).

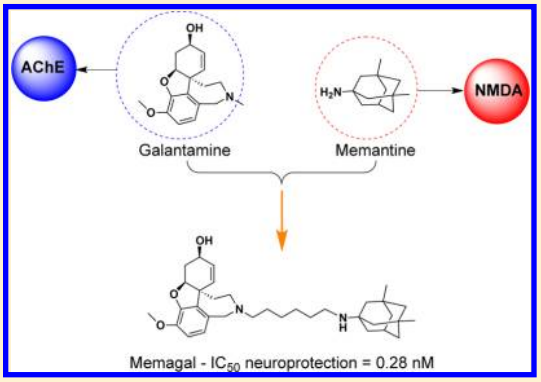

INTRODUCTION

Alzheimer's disease (AD) is a progressive and fatal brain disorder that causes memory loss, steady deterioration of cognition, and dementia. Over 30 million people worldwide are afflicted with the disease. It is estimated that, by 2050, there could be more than 100 million AD patients worldwide.[1] AD dramatically affects the quality of life of the sufferers and their families, and despite massive investments, there are few, if any, effective treatments for AD. The AD pathogenesis involves a complex interplay of genetic and biochemical factors, including an increased production of β-amyloid peptide (amyloid hypothesis) and an increased phosphorylation of the microtubule-associated tau protein (tau hypothesis).[2]

AD progression is associated with a significant disruption of several neurotransmitter systems, including the cholinergic, GABAergic, adrenergic, serotoninergic, and glutamatergic systems.[3] Alterations of cholinergic and glutamatergic systems have been extensively investigated,[4] leading to four acetylcholinesterase (AChE) inhibitors, donepezil, galantamine (**1**), rivastigmine, and tacrine (now discontinued) and one non-competitive *N*-methyl-D-aspartate (NMDA) receptor (NMDAR) antagonist, memantine (**2**, see Figure 1), which have been approved for use in AD patients. The current standard of care for AD is a combination of an AChE inhibitor with **2**.[5,6] The rationale for this approach is that the NMDAR antagonist will stop or delay neurodegeneration, while the AChE inhibitor will improve memory and cognition by stimulating the surviving neurons.

The usefulness of NMDAR antagonists in AD patients has been intensively debated over the years. It has long been known that NMDAR activation can be either beneficial, promoting neuronal survival, or detrimental, causing neuronal death.[7] The current consensus is that these opposite effects depend on receptor location: activation of postsynaptic NMDARs is beneficial, whereas activation of extrasynaptic NMDARs promotes neuronal death. This suggests that the latter receptor population should be the target for novel molecules.[7] In this respect, although **2** is far from being optimal, it is the only NMDAR antagonist in clinical use. This is probably because of its preferential action on the extrasynaptic NMDARs.[8]

Unlike other AChE inhibitor drugs, **1** has a postulated dual mechanism of action: in addition to inhibiting AChE, **1** has shown a facilitating effect on the nicotinic receptor-mediated transmission via allosteric modulation of the α-subunit of nicotinic receptors.[9] In particular, **1** can enhance synaptic

Received: July 4, 2012

dx.doi.org/10.1021/jm3009458 | J. Med. Chem. XXXX, XXX, XXX−XXX

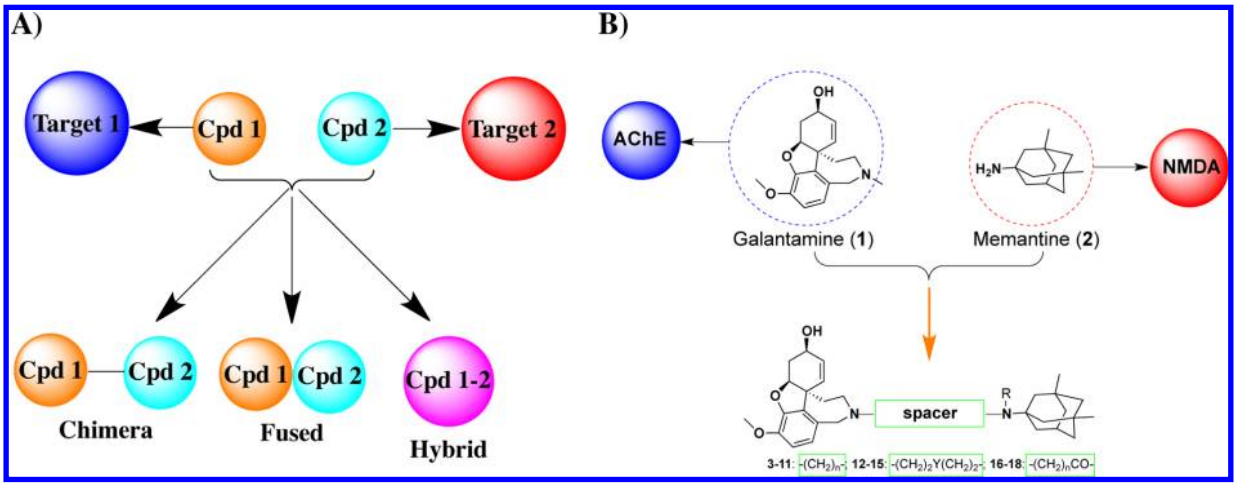

Figure 1. (A) Dual-target design strategy, according to Bottegoni et al.[20] In this study, we used the strategy of designing and synthesizing chimera derivatives of (B) galantamine (**1**) and memantine (**2**). Suitable spacers of different length and chemical composition were used, affording 16 new chemical entities, **3**–**18** (see Table 2).

NMDAR activity[10,11] by activating α7 nicotinic receptors located on presynaptic glutamatergic neurons.[12] Working together, **1** and **2** may thus improve neurophysiological responses in AD patients,[13] and their combination might offer a promising therapeutic strategy for AD treatment. **1** can provide the memory-enhancing activity of any AChE inhibitor, but it can also complement the effect of **2**.[14]

A possible alternative to drug combinations is to create molecules that can hit multiple targets; these are known as multitarget-directed ligands (MTDLs).[15] MTDLs are gaining increasing attention from the drug discovery community. Recent review articles have pointed out that the strategy of targeting two or more proteins with a single compound can provide therapeutic effects superior to those of a selective drug.[15−18] In addition, MTDLs can offer a number of potential benefits over cocktails or multicomponent drugs. These include the following: (i) reduced uncertainty in clinical development because predicting the pharmacokinetics of a single compound is much easier than with a drug cocktail; (ii) improved efficacy due to the synergistic effect of simultaneously inhibiting multiple targets; (iii) improved safety by decreasing the side effects related to the load of a drug cocktail with a reduced risk of drug−drug interactions; (iv) simplified therapeutic regimen and improved compliance, which is particularly important for elderly AD patients and their caregivers.[19]

In the present study, we combined in single new chemical entities the pharmacophoric moieties of **1** and **2** using our dual-target design strategy[20] schematically reported in Figure 1. The new chimera compounds were initially investigated by docking simulations, taking advantage of the crystallographic structure of AChE in complex with a bivalent derivative of **1**.[21] The spacers were designed to allow the new compounds to properly dock into the AChE gorge and to simultaneously contact both sites of the enzyme. In particular, different polymethylene spacers and heteroatoms were chosen (**3**−**8** and **12**−**15**). Moreover, we sought to evaluate the role of the adamantane amine function through the design of amide (**16**−**18**) and *N*-methyl (**9**−**11**) derivatives. In fact, the protonable nitrogen of **2** could establish cation−π interaction with the peripheral anionic site of AChE, thus increasing the affinity for this target. The molecules were then synthesized and tested against AChE and NMDAR. Interestingly, some of the new compounds showed an unexpected ability to interact with the NMDAR containing the 2B subunit of the receptor (hereafter referred to as NR2B), as they were able to displace ifenprodil, a selective NR2B ligand. It has been postulated that NR2B could be the major component of the extrasynaptic NMDAR population. Therefore, the neuroprotective profile of selected molecules was examined using SHSY-5Y cells.

RESULTS AND DISCUSSION

In this study, we investigated the feasibility of designing and synthesizing dual-target compounds, which were able to inhibit the AChE enzyme and to bind to the NMDAR. Other studies have previously sought to obtain dual AChE/NMDAR compounds.[22,23] However, for the first time, we combined in single new chemical entities two marketed drugs, **1** and **2** (see Figure 1 for the design strategy). Docking simulations demonstrated that the amine group of **1** was a suitable point to functionalize this fragment, which would afford compounds **3**−**18**. These compounds were then synthesized and biologically characterized.

Computational Design. Docking simulations were carried out to identify the proper length of the methylene linker connecting **1** to **2**. These simulations were performed on a model structure of AChE obtained by imposing, on the crystal structure of the human enzyme, the conformation adopted by its *Torpedo californica* orthologue in complex with a bivalent derivative of **1** (see the Experimental Section for further details). Table 1 reports the results of the docking simulations. Five to six methylenes were the minimal distance that allowed the new hybrid compounds to efficiently contact both sites (the internal and the peripheral anionic sites) of the AChE gorge without excessive strain on the linker. Interestingly, compounds with a linker length of six or seven units were characterized by an optimal balance between binding score and log *P*. Moreover, compounds with a six- or seven-methylene spacer displayed the most suitable distance between the basic adamantane amine and the indole ring of Trp286 to form a cation−π interaction. It is worth emphasizing that, due to its electronic nature, this specific interaction was not captured by the scoring function.

Figure 2 reports the binding mode of **6** at the AChE gorge. The galantamine part of the compound matched almost perfectly the crystallographic conformation, establishing a

dx.doi.org/10.1021/jm3009458 | J. Med. Chem. XXXX, XXX, XXX−XXX

Table 1. Outcomes of Docking Simulations Carried Out with Galantamine–Memantine Chimeras Containing Spacers of Different Length

compd	linker length	docking score (score units)	log *P*	ligand efficiency[a]	LELP[b]	cation–π distance[c] (Å)
3	4	−10.00	3.98	0.27	14.74	4.89
4	5	−13.38	4.46	0.35	12.67	4.91
5	6	−20.15	4.94	0.52	9.57	3.75
6	7	−22.03	5.42	0.55	9.84	3.40
7	8	−23.15	5.90	0.56	10.46	4.43
8	9	−18.72	6.38	0.44	14.33	4.76

[a]Ligand efficiency is expressed as Docking Score/no. of non-hydrogen atoms. [b]Ligand efficiency lipophilicity. [c]Distance between the protonated adamantan-1-amine and the center of the indole ring of Trp286.

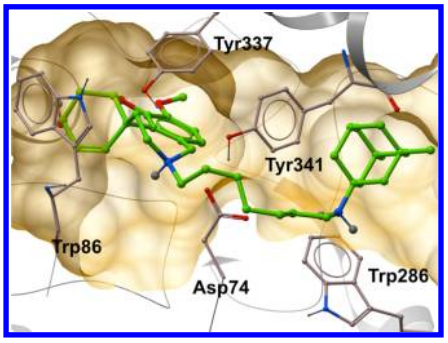

Figure 2. Bound conformation of **6** at the inner and peripheral anionic binding site of human AChE. The inhibitor is displayed in green, while the protein key residues are reported in gray and labeled explicitly. An orange mesh highlights the boundaries of the binding pocket.

hydrophobic interaction with the indole ring of Trp86 and donating a hydrogen bond to the side chain of Glu202. The linker was lodged in a narrow cavity described by Asp74, Tyr124, Phe297, Tyr337, Phe338, and Tyr341. The protonated nitrogen of the adamantane amine formed a cation–π interaction with the indole of Trp286. The adamatane moiety pointed toward the bulk of the solvent and established hydrophobic interaction with Val294, the backbone of Phe295, and the backbone of Gly342.

Chemical Syntheses. **3**–**18** were obtained following the synthetic approaches depicted in Schemes 1–3. Due to the easier chemical accessibility and availability of **2** with respect to desmethyl galantamine (**20**), the synthesis of **3**–**14** and **16**–**18** began by generating derivatives of **2**, **21**–**23**, **39**–**44**, **51**–**53**, and **63**–**65** as key intermediates, which were then connected to **20** (Schemes 1 and 2). The alkylation of **2** as hydrochloride salt with the appropriate bromo alcohol under basic conditions gave **24**–**30**. Then the amino group was Boc-protected, achieving **31**–**37**, which were treated with tosyl chloride to afford the easily substitutable tosyl-activated alcohols **38**–**44**. **38** was employed for the synthesis of **15** (Scheme 3), whereas **39**–**44** were subsequently reacted with **20**, providing compounds **45**–**50**. **3**–**8** were obtained in good yield after carbamate deprotection under mild acidic conditions to avoid degradation of the desired compounds (Scheme 1). **9**–**11** were synthesized starting from *N*-methylmemantine (**19**), which, in turn, was prepared through reductive methylation of the primary amine of **2** with aqueous formaldehyde and zinc dust by means of slight modification of a literature procedure.[24] The synthesis of **9**–**11** was accomplished by alkylation of **19** to furnish **21**–**23**, and the following activation of the alcohol group was achieved without isolation of the intermediates, which were directly reacted with **20** (Scheme 1). Amides **16**–**18** were easily prepared by a two-step procedure starting from **2** hydrochloride and the corresponding acylating agents. The resulting intermediates **51**–**53** were reacted with **20** to furnish **16**–**18** (Scheme 1). The introduction of heteroatom chains in **12**–**14** was carried out by selectively activating the appropriate dialcohol **54**–**56** (Scheme 2). The key intermediates **63**–**65** were prepared according to the procedure adopted for **38**–**44** and condensed with **20**, affording **66**–**68**. Then HCl-promoted deprotection of the amino group provided final compounds **12**–**14**. Because the above-described strategy failed for **15**, a convergent synthesis was performed by condensing **38** with **71**, which was derived from nucleophilic substitution between **20** and **69**. Finally, HCl-mediated removal of the Boc group furnished the target compound **15** (Scheme 3).

Biological Assays. All the compounds were tested to assess their abilities to inhibit AChE activity and bind to NMDAR. The AChE-inhibiting activities were measured using the classic method of Ellman.[25] Binding to NMDAR and NR2B-containing NMDAR was assessed using the assay based on the displacement of [^{3}H]MK-801 and [^{3}H]ifenprodil, respectively. In addition, the inhibition of the NMDA-mediated neurotoxicity (500 μM of NMDA for 6 h) was assessed using the SHSY-5Y neuroblastoma cell line.

Multitargeted Structure–Activity Relationships. All the compounds were initially tested to assess their ability to inhibit the two selected targets, AChE and NMDAR. Table 2 summarizes the biological data generated for compounds **3**–**18**. As reported above, **1** could be suitably modified at the amine function, because substituents at this position could fit into the AChE gorge and contact the peripheral anionic site of the enzyme, identified by the Trp286 residue (Figure 2). It has been extensively reported in the literature that compounds, which can simultaneously interact with both sites of AChE (internal and peripheral anionic sites), are expected to potently inhibit the enzyme.[26−32] According to these observations, we have discovered quite potent AChE inhibitors. In fact, **5**–**8**, which were able to interact with both sites of AChE (see Figure 2 and Supporting Information), were nanomolar inhibitors of this enzyme. In addition, the introduction of a methyl group on the nitrogen of **2** further improved the AChE-inhibiting potency, with **9** and **11** being the most potent AChE inhibitors of the present series (IC_{50} = 1.03 nM and 0.52 nM, respectively). Conversely, replacing methylenes of the spacer with heteroatoms (**12**–**15**) had a slight detrimental effect on the AChE-inhibiting potency (docking models of **12**–**18** in complex with AChE are reported in the Supporting Information). In addition, we also observed that "switching off" the charge on the moiety of **2**, by replacing the methylene close to the nitrogen with a carbonyl group, greatly affected the AChE-inhibiting profile. Docking simulations showed that the binding mode of the present series of compounds was quite well conserved (compare Figure 2 and the binding modes reported in Supporting Information), and therefore removal of the charge prevented **16**–**18** from properly interacting with Trp286 by means of a cation–π interaction, thus decreasing their affinity for the enzyme. Furthermore, reducing the chain length to four methylenes, as in compound **3**, prevented it from properly reaching Trp286 and significantly decreased its affinity (IC_{50} = 695.9 nM) when compared to **4**–**8**. All these data

dx.doi.org/10.1021/jm3009458 | J. Med. Chem. XXXX, XXX, XXX–XXX

Scheme 1. Synthesis of 3−11 and 16−18[a]

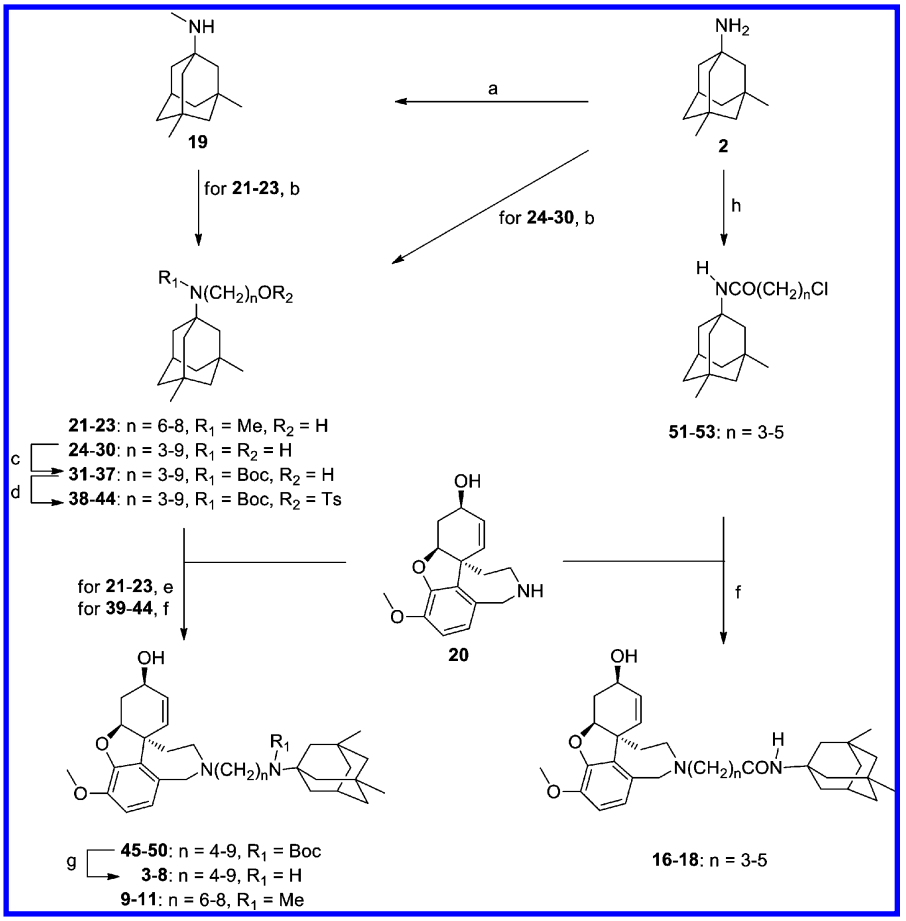

[a]Reagents and conditions: (a) CH_2O, MeCOOH, Zn, H_2O/dioxane, rt; (b) $HO(CH_2)_nBr$, K_2CO_3, DMF, 80 °C; (c) Boc_2O, Na_2CO_3, THF/H_2O, rt; (d) TsCl, Et_3N, DMAP, CH_2Cl_2, 0 °C to rt; (e) TsCl, Et_3N, DMAP, CH_2Cl_2, 0 °C to rt followed by **20**, Et_3N, MeCN, 80 °C; (f) Et_3N, MeCN, 80 °C; (g) 4 M HCl in dioxane, 0 °C to rt; (h) $ClCO(CH_2)_nCl$, MeCN, K_2CO_3, rt.

Scheme 2. Synthesis of 12−14[a]

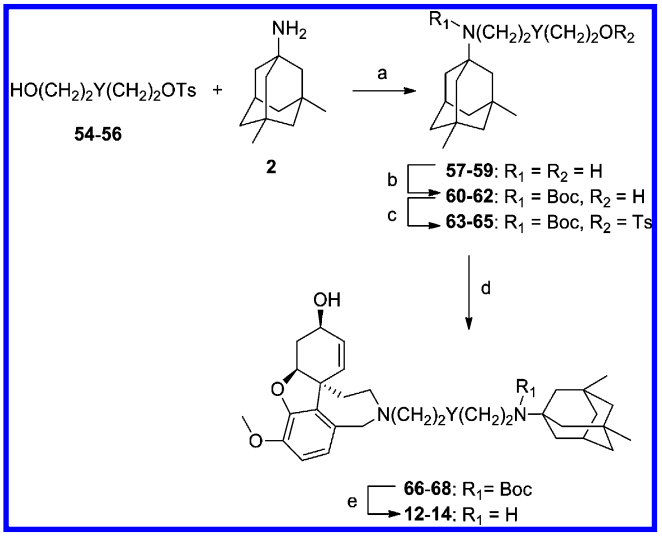

[a]Reagents and conditions: Y = $O(CH_2)_2O$; O; S; (a) K_2CO_3, DMF, 80 °C; (b) Boc_2O, Na_2CO_3, THF/H_2O, rt; (c) TsCl, Et_3N, DMAP, CH_2Cl_2, 0 °C to rt; (d) **20**, Et_3N, MeCN, 80 °C; (e) 4 M HCl in dioxane, 0 °C to rt.

Scheme 3. Synthesis of 15[a]

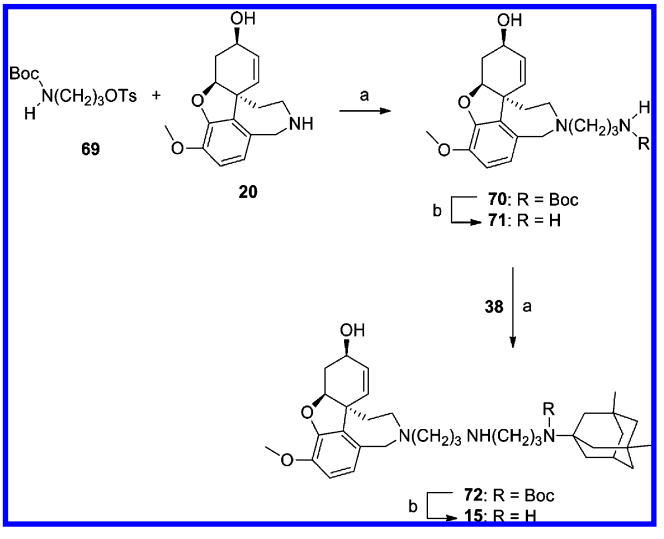

[a]Reagents and conditions: (a) Et_3N, MeCN, 80 °C; (b) 4 M HCl in dioxane, 0 °C to rt.

confirmed the binding mode reported in Figure 2 for the present series of chimeras.

As for NMDAR, some of the new compounds were active in the micromolar range (see Table 2), but none of the new derivatives was remarkably potent against this receptor. The

dx.doi.org/10.1021/jm3009458 | J. Med. Chem. XXXX, XXX, XXX−XXX

Table 2. Biological Activities of 3−18 against Rat AChE, NMDAR, NR2B, and the NMDA-Induced Neurotoxicity in Neuroblastoma Cell Lines

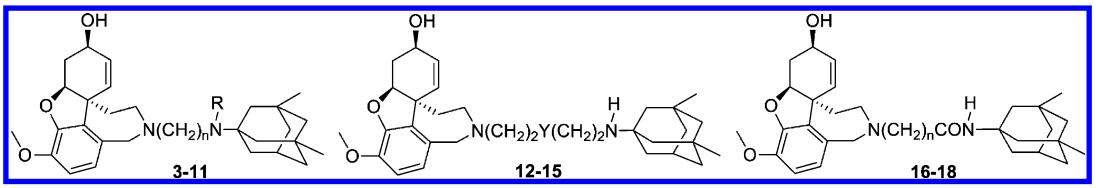

compd	*n*	R	Y	AChE, IC_{50} (nM)[c]	NMDAR [^{3}H] MK-801 binding assay[a], K_i (μM)[d]	NMDAR (NR2B) [^{3}H] ifenprodil binding assay[b], K_i (μM)[d]	SHSY-5Ycell viability assay, IC_{50} (nM) vs 500 μM NMDA[c]
3	4	H	–	695.9 ± 28.4	2.32 ± 0.43	>100	
4	5	H	–	4.31 ± 0.25	>10	40.9 ± 5.6	
5 (memagal)	6	H	–	1.16 ± 0.03	4.6 ± 0.6	4.6 ± 0.7	0.28 ± 0.05
6	7	H	–	1.79 ± 0.06	10.0 ± 2.1	10.95 ± 3.44	0.21 ± 0.02
7	8	H	–	5.36 ± 0.77	4.99 ± 0.20	2.9 ± 1.0	
8	9	H	–	2.32 ± 0.50	4.63 ± 1.54	>100	
9	6	CH_3	–	1.03 ± 0.18	>10	5.25 ± 1.6	
10	7	CH_3	–	1.33 ± 0.12	>10	>100	
11	8	CH_3	–	0.52 ± 0.05	>10	>100	
12	–	–	$O(CH_2)_2O$	80.9 ± 12.8	>10	>100	>10 000
13	–	–	O	3920 ± 690	>10	>100	
14	–	–	S	131.1 ± 29.5	>10	>100	
15	–	–	CH_2NHCH_2	167.8 ± 24.3	5.41 ± 1.11	3.32 ± 0.09	
16	3	–	–	55.7 ± 10.3	>10	>100	
17	4	–	–	369 ± 7.6	>10	>100	
18	5	–	–	11.3 ± 1.6	33.87 ± 4.73% at 10 μM[e]	9.76 ± 4.48	0.37 ± 0.04
1 (galantamine)				2550 ± 690	>10	>100	747 ± 67
2 (memantine)				8.50% ± 1.30 at 10 μM	1.16 ± 0.07	>100	718 ± 63
ifenprodil					3.08 ± 0.76	0.029 ± 0.0003	0.73 ± 0.04
MK801					K_d = 4.0 nM	>100	7.91 ± 0.45

[a]Displacement of specific [^{3}H]MK-801 binding in rat cortex membranes. [b]Displacement of specific [^{3}H]ifenprodil binding in rat cortex membranes. [c]A nonlinear multipurpose curve-fitting program, Prism (GraphPad Software Inc., San Diego, CA), was used for data analysis of rat AChE activity and cell viability; the IC_{50} value represents the compound concentration able to give 50% inhibition of rat AChE activity or NMDA-induced toxicity. Data are reported as the means ± SEM of three or four different experiments (performed in duplicate). [d]The K_i values are means ± SEM derived from an iterative curve-fitting procedure (Prism program, GraphPad, San Diego, CA). [e]Percentage of inhibition is reported for compound **18**.

affinity for this receptor appeared to be mainly driven by **2**, while the galantamine structure was not detrimental and did not cause any significant drop in affinity. In the MK-801 binding assay, the most potent derivative of the present series was **3**, showing a K_i value of 2.34 μM. In this case, the chain length did not affect the affinity against NMDAR (compare the potencies of **3**−**8**), while switching off the charge affected the affinities for this receptor (see compounds **16**−**18**), in agreement with previous observations.[33] The introduction of a methyl group on the nitrogen of **2** (**9**−**11**) had a detrimental effect on binding to NMDAR. Replacing methylenes of the spacer with heteroatoms (**12**−**15**) had a slight detrimental effect on the affinity for NMDAR. The only exception was **15**, where a methylene was replaced by an NH group. **15** showed a K_i value of 5.41 μM, comparable to that of the most potent derivative of the present series (**3**, K_i = 2.34 μM). As for **15**, we can hypothesize that a further protonable nitrogen, present on its spacer, can positively contribute to the recognition between the ligand and the channel that physiologically controls the permeation of bivalent positive cations.

In summary of the profiles against AChE and NMDAR, some of the new derivatives were nanomolar inhibitors of AChE, and micromolar binders of NMDAR. A comment is required here on the affinity-balancing issue.[34] The nanomolar profiles of the new compounds against AChE, along with the micromolar activities against NMDAR, call for a subsequent campaign of optimization to properly equalize the profile of **3**−**18** against the two targets. However, it should also be noted that, for in vivo efficacy, it is not strictly necessary that the two targets are modulated to the same extent. In the field of multitarget drug discovery, the issue of affinity-balancing is particularly challenging for the following two reasons: (i) increasing the affinity against the first target can decrease affinity against the second, and vice versa; (ii) there is the possibility that the two targets should be engaged to different extents (i.e., diverse target engagement profile) to provide optimal in vivo activity and efficacy. The latter aspect should be carefully considered when selecting two (or more) targets at the very early stages of a multitarget drug discovery program.

There is now compelling evidence that NR2B-containing NMDAR could preferentially contribute to pathologies linked to glutamate overexcitation.[35−37] Therefore, we turned our attention to NR2B, testing all the compounds using the ifenprodil binding assay (see the Experimental Section for details). While most of the compounds were unable to displace ifenprodil (see Table 2), some of the new derivatives (compounds **5**−**7**, **9**, **15**, and **18**) showed K_i values in the micromolar range. A comment is required here on the SAR of the present series of compounds against NR2B-containing NMDAR. In fact, we noticed that slight structural modifications

dx.doi.org/10.1021/jm3009458 | J. Med. Chem. XXXX, XXX, XXX−XXX

caused a drop in affinity for NR2B-containing NMDAR. To rationalize such a behavior, we carried out docking simulations using the crystal structure of NR2B in complex with ifenprodil (see Experimental Section for details). In the Supporting Information, we report the docking model of NR2B in complex with **5**. The compound fitted quite well into the infenprodil binding pocket, establishing relevant hydrophobic and H-bond interactions (for a detailed description of all interactions, see the Supporting Information). The proposed binding mode could explain the good affinity of **5** for NR2B (K_i = 4.6 μM), as well as the ability of the compound to displace ifenprodil as experimentally observed. However, the SARs for this receptor subunit remained puzzling and difficult to be properly rationalized on the basis of our docking model. Further studies are required to properly generate meaningful SARs for the present series of derivatives against NR2B-containing NMDAR.

These encouraging data prompted us to test some representative compounds using a cell-based assay to assess their neuroprotective profile against NMDA-mediated neurotoxicity. SHSY-5Y cells were treated with 500 μM NMDA for 6 h in the absence or presence of different concentrations of selected compounds, to generate the dose−response curves of inhibition of the NMDA-induced neurotoxicity. Compounds **5**, **6**, and **18** were remarkably potent in these experimental conditions, as they were able to inhibit NMDA-induced neurotoxicity with subnanomolar potencies. In particular, **6** showed an IC_{50} value of 0.21 nM, while **5** (which we named memagal) and **18** showed IC_{50} values of 0.28 nM and 0.37 nM, respectively. As negative control, we tested **12** (NR2B K_i > 100 μM), which started to inhibit NMDA neurotoxicity at 10 μM. Other compounds could not be tested up to 10 μM, because they were cytotoxic at this concentration. Under the same conditions, we also tested **2**, which affected cell viability at a much higher concentration (718 nM; see Table 2). These cell-based data were extremely promising and not fully explained by the binding potencies (in the micromolar range) of these compounds against NR2B. Interestingly, while a nanomolar antagonist of NMDAR unable to bind to NR2B (i.e., MK-801; see Table 2) inhibited the NMDA-induced toxicity at nanomolar concentration (IC_{50} = 7.91 nM), a selective nanomolar ligand of NR2B (ifenprodil) exerted the same effect at a subnanomolar concentration (IC_{50} = 0.73 nM). Similarly, we observed that our compounds, which displaced both MK-801 and ifenprodil at micromolar concentrations, were able to inhibit NMDA-induced neurotoxicity in the subnanomolar range. A possible explanation for this behavior could be that nonselective binders, able to displace both MK-801 and ifenprodil, could result in potent neuroprotective agents, due to possible synergistic and/or additive effects.

CONCLUSIONS

In AD, there is still a need for drugs that simultaneously stimulate the cholinergic system while suppressing glutamate neurotoxicity, providing molecules endowed with neuroprotective profiles. In light of the recent failures of compounds that block targets belonging to the amyloid and the tau cascades, there is interest in broadening efficacy of anticholinesterase drugs, by contrasting the progressive neurodegeneration responsible for their decline in efficacy. The neuroprotective profile, achieved through modulating NMDARs, can lengthen the time in which anticholinesterase drugs can provide beneficial effects on memory and cognition. With this in mind, we designed and synthesized novel multitargeted compounds obtained by chemically combining **1** and **2**, two marketed drugs for the treatment of AD. Our molecules turned out to be remarkably active against AChE with the most potent derivative showing an IC_{50} value of 0.52 nM. For NMDAR, we obtained micromolar binders. The most potent derivative (**3**) showed a K_i of 2.32 μM against NMDAR. However, it was slightly more potent against AChE (IC_{50} = 695.9 nM). This series of molecules has further highlighted the inherent difficulty of balancing the affinity profiles against diverse targets, when discovering and developing MTDLs. The molecules were then tested against NR2B-containing NMDAR, using the ifenprodil binding assay. A few compounds were active in the micromolar range, with **7** being the most potent binder of NR2B (K_i = 2.9 μM). These molecules are the first ever derivatives reported to show a dual AChE/NR2B profile. They could be promising tools for investigating the simultaneous modulation of these two targets in AD. Finally, in light of the NR2B profile, selected derivatives were tested using cellular assays, to investigate the neuroprotective profile after insult by NMDA. While most of the derivatives were inactive or cytotoxic at micromolar concentration, compounds **5**, **6**, and **18** turned out to be subnanomolar inhibitors of the NMDA-mediated neurotoxicity. The high potencies of these molecules as neuroprotective agents might lie in their ability to nonselectively modulate NMDARs. This intriguing biological profile deserves further investigation as it could open up new avenues for generating leads and drug candidates endowed with optimal anticholinesterase and neuroprotective profiles against AD.

EXPERIMENTAL SECTION

Chemical Synthesis. *Chemistry.* Chemical reagents were purchased from Sigma Aldrich, Fluka (Italy), and TCI-Europe. *N*-Desmethylgalantamine was purchased from Synfine research. Solvents were RP grade. Dichloromethane was distilled from calcium chloride. Dry dimethylformamide and triethylamine were used as supplied. Nuclear magnetic resonance spectra (NMR) were recorded at 400 MHz on Varian VXR 400 spectrometers and reported in parts per million. All final compounds **3**−**18** are >95% pure by UPLC-MS analyses. The analyses were performed on a Waters ACQUITY UPLC-MS instrument consisting of an SQD single quadropole mass spectrometer equipped with an electrospray ionization interface and a photodiode array detector. The analyses were performed on an ACQUITY UPLC BEH C18 column (50 × 2.1 mm ID, particle size 1.7 μm) with a VanGuard BEH C18 precolumn (5 × 2.1 mm ID, particle size 1.7 μm). The mobile phases were 10 mM NH_4OAc at pH 5 adjusted with AcOH (A) and 10 mM NH_4OAc in MeCN−H_2O (95:5) at pH 5 (B). Linear Gradient: 0−0.2 min, 10% B; 0.2−6.2 min, 10−90% B; 6.2−6.3 min, 90−100% B; 6.3−7 min, 100% B; at a flow rate of 0.5 mL/min. Electrospray ionization in positive and negative mode was used in the mass scan range 100−500 Da. Optical rotations were measured on a Rudolf Research Analytical Autopol II Automatic polarimeter using a sodium lamp (589 nm) as the light source; concentrations expressed in g/100 mL using $CHCl_3$ as a solvent and a 1 dm cell. Column chromatography purifications were performed under "flash conditions" using Sigma Aldrich silica gel grade 9385, 230−400 mesh. TLC were performed on 0.20 mm silica gel 60 F254 plates (Merck, Germany), which were visualized by exposure to ultraviolet light and potassium permanganate stain. Reactions involving generation or consumption of amine were visualized by using

dx.doi.org/10.1021/jm3009458 | J. Med. Chem. XXXX, XXX, XXX−XXX

bromocresol green spray (0.04% in EtOH made blue by NaOH) following heating of the plate. Compounds were named following IUPAC rules as applied by Beilstein-Institute AutoNom (version 2.1), a PC integrated software package for systematic names in organic chemistry.

*N,3,5-Trimethyladamantan-1-amine (**19**).* Glacial acetic acid (0.382 mL, 6.66 mmol), Zn dust (0.436 g, 6.66 mmol), and 35% aqueous formaldehyde (0.833 mL, 16.65 mmol) were sequentially added to a solution of **2** hydrochloride (0.720 g, 3.33 mmol) in dioxane/H_2O (1:1). The mixture was stirred at 30 °C for 2 days. Then, saturated NH_4Cl aqueous solution was added (5 mL), and the resulting mixture extracted with CH_2Cl_2 (3 × 10 mL). The combined organic layers were then washed with brine and dried over Na_2SO_4. The crude product was purified by flash chromatography (CH_2Cl_2/MeOH/33% aqueous NH_3 9:1:1.8) to achieve **19** as a white solid: 0.480 g (75%). ^{1}H NMR ($CDCl_3$, 400 MHz) δ 0.76 (s, 6H), 1.04−1.05 (AB m, 2H), 1.15−1.23 (m, 8H), 1.40−1.41 (m, 2H), 2.05−2.07 (m, 1H), 2.26 (s, 3H), 2.75 (br s, exchangeable with D_2O, 1H).

*General Procedure for the Synthesis of **54**−**56**.* *p*-TsCl (1.2 equiv) was added dropwise to a mixture of the appropriate diol (1 equiv), Et_3N (1 equiv), and DMAP (catalytic amount) in dry CH_2Cl_2 (0.01 M) under N_2 atm, with stirring at 0 °C. The stirring was continued at room temperature for 4 h. The reaction was quenched with saturated NH_4Cl aqueous solution, and the whole was extracted with AcOEt. The extract was washed with brine and dried over Na_2SO_4, and, following solvent evaporation, the crude material was purified by flash chromatography (see Supporting Information for details).

*General Procedure for the Synthesis of **21**−**30** and **57**−**59**.* In a pressure tube (Sigma Aldrich, ACE pressure tube) the appropriate bromo alcohol or the activated alcohol **54**−**56** (1.2 equiv) was added to a vigorously stirred solution of **19** (1 equiv) or **2** hydrochloride (1 equiv) and K_2CO_3 (2.5 equiv) in DMF (0.2 M). The reaction mixture was stirred at 80 °C for 48 h. After evaporation of the solvent, the residue was taken up with water and extracted with CH_2Cl_2 (3 × 10 mL). The collected organic layers were concentrated, and the crude was purified by flash chromatography (see Supporting Information for details).

*General Procedure for the Synthesis of **31**−**37** and **60**−**62**.* The appropriate secondary amine (1 equiv) was dissolved in THF/H_2O (2:1) and treated with Na_2CO_3 (2.5 equiv) and di-*tert*-butyl dicarbonate (1.5 equiv). The resulting suspension was stirred at room temperature overnight. The solvent was then removed in vacuo, yielding a residue, which was dissolved in water and extracted with AcOEt (3 × 15 mL). The extracts were combined, washed with brine, dried over Na_2SO_4, concentrated, and purified by flash chromatography (see Supporting Information for details).

*General Procedure for the Synthesis of **38**−**44** and **63**−**65**.* *p*-TsCl (1 equiv) was added to a mixture of the appropriate alcohol (1 equiv), Et_3N (2 equiv), and DMAP (catalytic amount) in dry CH_2Cl_2 (0.1 M) under N_2 atmosphere, with stirring at 0 °C. The stirring was continued at room temperature for 3.5 h. After completion, the reaction was quenched with saturated NH_4Cl aqueous solution and extracted with AcOEt (3 × 10 mL). Combined extracts were washed with brine, dried over Na_2SO_4, and evaporated. The tosylate derivative was then purified by flash chromatography (see Supporting Information for details).

*General Procedure for the Synthesis of **45**−**50** and **66**−**68**.* A mixture of the appropriate activated alcohol (1.2 equiv), **20** (1 equiv) and Et_3N (2 equiv) in MeCN (0.1 M) was stirred at 80 °C for 48 h in a pressure tube. After evaporation of the solvent, the residue was purified by flash chromatography (see Supporting Information for details).

*General Procedure for the Synthesis of **3**−**8** and **12**−**14**.* HCl (4 M) in dioxane (1 mL) was carefully added to the appropriate Boc derivative (1 equiv) at 0 °C. The resulting solution was stirred at room temperature for 2 h. After removal of the solvent,, the obtained residue was purified by flash chromatography.

*(4aS,6R,8aS)-11-(4-((3,5-Dimethyladamantan-1-yl)-amino)butyl)-3-methoxy-5,6,9,10,11,12-hexahydro-4aH-benzo[2,3]benzofuro[4,3-cd]azepin-6-ol (**3**).* **3** was synthesized from **45** (0.066 g, 0.11 mmol). Elution with CH_2Cl_2/CH_3OH/33% aqueous ammonia (9:1:0.1) afforded **3** as a waxy solid: 0.050 g (91%). ^{1}H NMR ($CDCl_3$, 400 MHz) δ 0.84 (s, 6H), 1.08−1.16 (AB m, 2H), 1.25−1.37 (m, 9 H), 1.52−1.61 (m, 6H), 1.98−2.09 (m, 2H), 2.13−2.14 (m, 1H), 2.48−2.58 (m, 2H), 2.61−2.71 (m, 3H), 3.19−3.33 (2H), 3.82 (AB d, J = 15.2, 1H), 3.83 (s, 3H), 4.10−4.13 (m+AB d, J = 15.2 Hz, 2H), 4.60 (br m, 1H), 6.00 (dd, J_1 = 10.4, Hz, J_2 = 4.8 Hz, 1H), 6.07 (d, J = 10.4 Hz, 1H), 6.63 (d, J = 8.0, 1H), 6.66 (d, J = 8.0, 1H). ^{13}C NMR ($CDCl_3$, 100 MHz) δ 25.27, 27.91, 29.67, 29.92, 30.06, 30.16, 32.37, 33.01, 40.28, 42.70, 47.69, 48.32, 50.65, 51.46, 51.81, 55.85, 57.62, 62.02, 88.71, 111.19, 122.14, 126.75, 127.70, 128.80, 133.13, 144.17, 145.83. $[\alpha]^{25}_D$ = −57.4 (*c* 0.07, $CHCl_3$). UPLC/MS: purity 97%, MS (ESI+): *m*/*z* 507.4 $[M + H]^+$.

*(4aS,6R,8aS)-11-(5-((3,5-Dimethyladamantan-1-yl)-amino)pentyl)-3-methoxy-5,6,9,10,11,12-hexahydro-4aH-benzo[2,3]benzofuro[4,3-cd]azepin-6-ol (**4**).* **4** was synthesized from **46** (0.170 g, 0.27 mmol). Elution with CH_2Cl_2/CH_3OH/33% aqueous ammonia (9:1:0.1) afforded **4** as a waxy solid: 0.095 g (66%). ^{1}H NMR ($CDCl_3$, 400 MHz) δ 0.84 (s, 6H), 1.11−1.21 (AB m, 2H), 1.26−1.35 (m, 11 H), 1.46−1.52 (m, 6H), 1.98−2.03 (m, 2H), 2.13−2.14 (m, 1H), 2.42−2.50 (m, 2H), 2.59 (t, J = 7.6, 2H), 2.66−2.71 (m, 1H), 3.16−3.17 (1H), 3.33−3.34 (m, 1H), 3.79 (AB d, J = 15.2, 1H), 3.83 (s, 3H), 4.10−4.13 (m+AB d, J = 15.2 Hz, 2H), 4.60 (br m, 1H), 6.00 (dd, J_1=10.4, Hz, J_2 = 4.8 Hz, 1H), 6.08 (d, J = 10.0 Hz, 1H), 6.60 (d, J = 8.4, 1H), 6.65 (d, J = 8.4, 1H). ^{13}C NMR ($CDCl_3$, 100 MHz) δ 25.14, 27.25, 29.94, 30.17, 30.23, 32.37, 32.94, 40.43, 42.85, 48.41, 50.79, 51.52, 55.88, 57.76, 62.07, 88.71, 111.13, 121.97, 126.96, 127.53, 129.52, 133.14, 144.03, 144.77. $[\alpha]^{25}_D$ = −63.2 (*c* 0.05, $CHCl_3$). UPLC/MS: purity 97%, MS (ESI+): *m*/*z* 521.6 $[M + H]^+$.

*(4aS,6R,8aS)-11-(6-((3,5-Dimethyladamantan-1-yl)-amino)hexyl)-3-methoxy-5,6,9,10,11,12-hexahydro-4aH-benzo[2,3]benzofuro[4,3-cd]azepin-6-ol (**5**).* **5** was synthesized from **47** (0.160 g, 0.25 mmol). Elution with CH_2Cl_2/CH_3OH/33% aqueous ammonia (9:1:0.1) afforded **5** as a waxy solid: 0.075 g (56%). ^{1}H NMR ($CDCl_3$, 400 MHz) δ 0.84 (s, 6H), 1.09−1.15 (AB m, 2H), 1.18−1.37 (m, 11H), 1.42−1.54 (m, 8H), 1.98−2.04 (m, 2H), 2.13−2.14 (m, 1H), 2.42−2.51 (m, 2H), 2.60 (t, J = 7.6, 2H), 2.66−2.71 (m, 1H), 3.16−3.17 (1H), 3.31−3.33 (m, 1H), 3.79 (AB d, J = 16.0, 1H), 3.83 (s, 3H), 4.10−4.13 (m+AB d, J = 16.0 Hz, 2H), 4.60 (br m, 1H), 6.00 (dd, J_1 = 10.4, Hz, J_2 = 4.8 Hz, 1H), 6.08 (d, J = 10.0 Hz, 1H), 6.60 (d, J = 8.4, 1H), 6.65 (d, J = 8.4, 1H). ^{13}C NMR ($CDCl_3$, 100 MHz) δ 22.66, 26.67, 27.21, 27.38, 29.67, 29.94, 30.14, 30.21, 31.89, 32.38, 32,95, 33.66, 40.45, 42.80, 47.95,

dx.doi.org/10.1021/jm3009458 | *J. Med. Chem.* XXXX, XXX, XXX−XXX

48.41, 50.74, 51.50, 53.66, 55.85, 55.88, 57.77, 62.07, 88.70, 111.11, 121.97, 126.97, 127.51, 129.56, 133.15, 144.00. 145.76. $[\alpha]^{25}_{D}$ = −34.9 (*c* 0.10, $CHCl_3$). UPLC/MS: purity 100%, MS (ESI+): *m/z* 535.6 $[M + H]^+$.

*(4aS,6R,8aS)-11-(7-((3,5-Dimethyladamantan-1-yl)-amino)heptyl)-3-methoxy-5,6,9,10,11,12-hexahydro-4aH-benzo[2,3]benzofuro[4,3-cd]azepin-6-ol (**6**).* **6** was synthesized from **48** (0.130 g, 0.20 mmol). Elution with CH_2Cl_2/CH_3OH (9:1) afforded **6** as a waxy solid: 0.070 g (64%). ^1H NMR ($CDCl_3$, 400 MHz) δ 0.84 (s, 6H), 1.08−1.15 (AB m, 2H), 1.23−1.34 (m, 15H), 1.44−1.51 (m, 6H), 1.94−2.07 (m, 2H), 2.13 (br m, 1H), 2.40−2.52 (m, 2H), 2.57 (t, *J* = 7.2 Hz, 2H), 2.66−2.69 (m, 1H), 3.14−3.18 (1H), 3.31−3.37 (m, 1H), 3.79 (AB d, *J* = 15.2, 1H), 3.83 (s, 3H), 4.09−4.15 (m+AB d, *J* = 15.2 Hz, 2H), 4.60 (br m, 1H), 5.99 (dd, J_1 = 10.4, Hz, J_2 = 4.8 Hz, 1H), 6.08 (d, *J* = 10.0 Hz, 1H), 6.61 (d, *J* = 8.4, 1H), 6.65 (d, *J* = 8.4, 1H). ^{13}C NMR ($CDCl_3$, 100 MHz) δ 27.35, 27.50, 27.55, 27.72, 29.40, 29.91, 30.05, 30.16, 32.14, 32.72, 33.19, 38.29, 40.36, 42.46, 45.58, 48.64, 50.41, 51.74, 56.11, 57.25, 58.02, 62.31, 88.94, 111.37, 122.21, 127.21, 127.77, 129.74, 133.39, 144.25, 146.01. $[\alpha]^{25}_{D}$ = −64.1 (*c* 0.11, $CHCl_3$). UPLC/MS: purity 100%, MS (ESI+): *m/z* 549.6 $[M + H]^+$.

*(4aS,6R,8aS)-11-(8-((3,5-Dimethyladamantan-1-yl)-amino)octyl)-3-methoxy-5,6,9,10,11,12-hexahydro-4aH-benzo[2,3]benzofuro[4,3-cd]azepin-6-ol (**7**).* **7** was synthesized from **49** (0.160 g, 0.24 mmol). Elution with CH_2Cl_2/CH_3OH (9:1) afforded **7** as a waxy solid: 0.093 g (68%). ^1H NMR ($CDCl_3$, 400 MHz) δ 0.86 (s, 6H), 1.14−1.15 (AB m, 2H), 1.22−1.37 (m, 13H), 1.43−1.53 (m, 7H), 1.64−1.68 (m, 4H), 1.98−2.05 (m, 2H), 2.16−2.17 (m, 1H), 2.43−2.49 (m, 2H), 2.66−2.70 (m, 2H), 3.16−3.17 (m, 1H), 3.29−3.35 (m, 1H), 3.79 (AB d, *J* = 15.2, 1H), 3.83 (s, 3H), 4.10−4.15 (m +AB d, *J* = 15.2 Hz, 2H), 4.61 (br m, 1H), 6.00 (dd, J_1 = 10.4, Hz, J_2= 4.8 Hz, 1H), 6.08 (d, *J* = 10.0 Hz, 1H), 6.61 (d, *J* = 8.4, 1H), 6.66 (d, *J* = 8.4, 1H). ^{13}C NMR($CDCl_3$, 100 MHz) δ 27.27, 27.30, 27.40, 29.25, 29.51, 29.66, 29.94, 30.06, 32.42, 32.97, 40.18, 42.48, 46.21, 50.43, 51.46, 55.84, 55.90, 58.60, 62.07, 88.74, 111.12, 121.97, 126.97, 127.53, 129.51, 133.15, 144.01, 145.77, 177.21. $[\alpha]^{25}_{D}$ = −63.5 (*c* 0.12, $CHCl_3$). UPLC/MS: purity 100%, MS (ESI+): *m/z* 563.4 $[M + H]^+$.

*(4aS,6R,8aS)-11-(9-((3,5-Dimethyladamantan-1-yl)-amino)nonyl)-3-methoxy-5,6,9,10,11,12-hexahydro-4aH-benzo[2,3]benzofuro[4,3-cd]azepin-6-ol (**8**).* **8** was synthesized from **50** (0.095 g, 0.14 mmol). Elution with CH_2Cl_2/CH_3OH (9:1) afforded **8** as a waxy solid: 0.060 (75%). ^1H NMR ($CDCl_3$, 400 MHz) δ 0.85 (s, 6H), 1.11−1.14 (AB m, 2H), 1.26−1.59 (m, 25 H), 1.98−2.09 (m, 2H), 2.16−2.17 (m, 1H), 2.40−2.53 (m, 2H), 2.60−2.71 (m, 3H), 3.15−3.18 (m, 1H), 3.21−3.37 (m, 1H), 3.79 (AB d, *J* = 15.2, 1H), 3.83 (s, 3H), 4.10−4.14 (m+AB d, *J* = 15.2 Hz, 2H), 4.61 (br m, 1H), 6.00 (dd, J_1= 10.4 Hz, J_2= 4.8 Hz, 1H), 6.10 (d, *J* = 10.0 Hz, 1H), 6.61 (d, *J* = 8.4, 1H), 6.65 (d, *J* = 8.4, 1H). ^{13}C NMR ($CDCl_3$, 100 MHz) δ 27.35, 27.45, 29.40, 29.48, 29.52, 29.95, 30.12, 30.19, 32.40, 32.98, 40.56, 42.76, 48.41, 50.70, 51.50, 55.87, 57.82, 62.07, 88.71, 111.10, 121.95, 126.98, 127.51, 129.62, 133.15, 143.10, 145.77. $[\alpha]^{25}_{D}$ = −57.2 (*c* 0.10, $CHCl_3$). UPLC/MS: purity 99%, MS (ESI+): *m/z* 577.6 $[M + 1]^+$.

*(4aS,6R,8aS)-11-(2-(2-(2-((3,5-Dimethyladamantan-1-yl)-amino)ethoxy)ethoxy)ethyl)-3-methoxy-5,6,9,10,11,12-hexahydro-4aH-benzo[2,3]benzofuro[4,3-cd]azepin-6-ol (**12**).* **12** was synthesized from **66** (0.080 g, 0.12 mmol). Elution with CH_2Cl_2/CH_3OH/33% aqueous ammonia (9:1:0.05) afforded **12** as a waxy solid: 0.060 g (88%). ^1H NMR ($CDCl_3$, 400 MHz) δ 0.84 (s, 6H), 1.08−1.16 (AB m, 2H), 1.26−1.37 (m, 8H), 1.51−1.54 (m, 3H), 1.98−2.09 (m, 2H), 2.15 (br m, 1H), 2.66−2.70 (m, 1H), 2.74 (t, *J* = 5.8 Hz, 2H), 2.83 (t, *J* = 4.8 Hz, 2H), 3.21−3.25 (m, 1H), 3.38−3.44 (m, 1H), 3.54−3.67 (m, 8H), 3.83 (s, 3H), 3.88 (d, *J* = 15.2 Hz, 1H), 4.13−4.15 (m, 1H), 4.18 (d, *J* = 15.2 Hz, 1H), 4.60 (br m, 1H), 6.00 (dd, J_1 = 10.4, J_2 = 5.2 Hz, 1H), 6.08 (d, *J* = 10.4 Hz, 1H), 6.61 (d, *J* = 8.0 Hz, 1H), 6.65 (d, *J* = 8.4 Hz, 1H). ^{13} C NMR($CDCl_3$, 100 MHz) δ 29.92, 30.12, 30.18, 32.38, 32.91, 40.05, 40.29, 42.77, 47.95, 48.40, 50.72, 51.83, 55.87, 57.89, 62.03, 68.99, 70.04, 70.16, 70.27, 88.68, 111.17, 122.21, 126.80, 127.63, 129.22, 133.14, 144.12, 145.82. $[\alpha]^{25}_{D}$ = −45.4 (*c* 0.11, $CHCl_3$). UPLC/MS: purity 99%, MS (ESI+): *m/z* 567.5 $[M + 1]^+$.

*(4aS,6R,8aS)-11-(2-(2-((3,5-Dimethyladamantan-1-yl)-amino)ethoxy)ethyl)-3-methoxy-5,6,9,10,11,12-hexahydro-4aH-benzo[2,3]benzofuro[4,3-cd]azepin-6-ol (**13**).* **13** was synthesized from **67** (0.115 g, 0.18 mmol). Elution with CH_2Cl_2/CH_3OH/33% aqueous ammonia (9:1:0.05) afforded **13** as a waxy solid: 0.085 g (88%). ^1H NMR ($CDCl_3$, 400 MHz) δ 0.87 (s, 6H), 1.11−1.01 (AB m, 2H), 1.24−1.33 (m, 4H), 1.36−1.45 (AB m, 4H), 1.54−1.62 (m, 3H), 1.98−2.11 (m, 2H), 2.20 (br m, 1H), 2.66−2.71 (m, 1H), 2.76 (t, *J* = 5.2 Hz, 2H), 2.90 (t, *J* = 4.8 Hz, 2H), 3.34−3.39 (m, 2H), 3.53−3.62 (m, 2H), 3.71−3.72 (m, 2H), 3.83 (s, 3H), 3.95 (d, *J* = 15.2 Hz, 1H), 4.14−4.17 (m+d, *J* = 15.2 Hz, 2H), 4.61 (br m, 1H), 6.00−6.08 (m, 2H), 6.65−6.67 (m, 2H).^{13} C NMR ($CDCl_3$, 100 MHz) δ 30.06, 32.58, 40.34, 42.55, 48.35, 50.50, 51.54, 55.87, 57.30, 62.00, 88.70, 111.27, 122.38, 126.52, 127.86, 133.10, 144.28, 145.83. $[\alpha]^{25}_{D}$ = −65.3 (*c* 0.10, $CHCl_3$). UPLC/MS: purity 95%, MS (ESI+): *m/z* 523.4 $[M + H]^+$.

*(4aS,6R,8aS)-11-(2-((2-((3,5-Dimethyladamantan-1-yl)-amino)ethyl)thio)ethyl)-3-methoxy-5,6,9,10,11,12-hexahydro-4aH-benzo[2,3]benzofuro[4,3-cd]azepin-6-ol (**14**).* **14** was synthesized from **68** (0.075 g, 0.12 mmol). Elution with CH_2Cl_2/CH_3OH/33% aqueous ammonia (9:1:0.05) afforded **14** as a waxy solid: 0.055 g (88%). ^1H NMR ($CDCl_3$, 400 MHz) δ 0.82 (s, 6H), 1.04−1.13 (AB m, 2H), 1.19−1.27 (m, 6H), 1.43 (br s, 2H), 1.48−1.51 (m, 1H), 1.98−2.04 (m, 2H), 2.09−2−11(m, 1H), 2.59−2.75 (m, 8H), 3.15 (m, 1H), 3.18 (m, 1H), 3.36−3.42 (m, 1H), 3.60−3.64 (m, 1H), 3.72−3.76 (m, 1H), 3.81 (s, 3H), 3.82 (d, *J* = 15.2 Hz, 1H), 4.10−4.17 (m +d, *J* = 15.2 Hz, 2H), 4.58 (br m, 1H), 5.99 (dd, J_1 = 10.0, J_2 = 4.4 Hz, 1H), 6.05 (d, *J* = 10.0 Hz, 1H), 6.58 (d, *J* = 8.4 Hz, 1H), 6.63 (d, *J* = 8.4 Hz, 1H). ^{13} C NMR ($CDCl_3$, 100 MHz) δ 29.67, 29.86, 29.93, 30.25, 30.30, 32.37, 33.00, 33.68, 39.65, 41.27, 42.85, 42.97, 48.41, 49.00, 49.04, 50.91, 51.70, 52.25, 55.89, 57.38, 62.03, 71.11, 72.29, 88.69, 111.17, 121.94, 126.74, 127.69, 129.15, 133.07, 144.20, 145.90. $[\alpha]^{25}_{D}$ = −68.7 (*c* 0.09, $CHCl_3$) UPLC/MS: purity 97%, MS (ESI+): *m/z* 539 $[M + H]^+$.

*General Procedure for the Synthesis of **9**−**11**.* *p*-TsCl (1 equiv) was added to a mixture of the appropriate alcohol (1 equiv), Et_3N (2 equiv), and DMAP (catalytic amount) in dry CH_2Cl_2 (0.1 M) under N_2 atmosphere, with stirring at 0 °C. The stirring was continued at room temperature for 3.5 h. After completion, the reaction was quenched with saturated NH_4Cl aqueous solution and extracted with AcOEt (3 × 10 mL). Combined extracts were washed with brine, dried over Na_2SO_4, and evaporated to give a residue that was transferred into a pressure tube. **20** (0.5 equiv) and Et_3N (2 equiv) in MeCN

dx.doi.org/10.1021/jm3009458 | J. Med. Chem. XXXX, XXX, XXX−XXX

were added, and the resulting mixture was stirred at 80 °C for 48 h. After evaporation of the solvent, the residue was purified by flash chromatography.

*(4aS,6R,8aS)-11-(6-((3,5-Dimethyladamantan-1-yl)-(methyl)amino)hexyl)-3-methoxy-5,6,9,10,11,12-hexahydro-4aH-benzo[2,3]benzofuro[4,3-cd]azepin-6-ol (**9**).* **9** was synthesized from **21** (0.210 g, 0.72 mmol). Elution with CH_2Cl_2/CH_3OH/33% aqueous ammonia (9:1:0.15) afforded **9** as a waxy solid: 0.085 g (43%). ^{1}H NMR ($CDCl_3$, 400 MHz) δ 0.87 (s, 6H), 1.08−1.17 (AB m, 2H), 1.24−1.33 (m, 9H), 1.38−1.52 (m, 7H), 1.60−1.65 (m, 3H), 1.98−2.07 (m, 2H), 2.19 (br m, 1H), 2.35 (s, 3H), 2.41−2.53 (m, 4H), 2.67−2.71 (m, 1H), 3.11−3.18 (m, 1H), 3.31−3.38 (m, 1H), 3.80 (AB d, J = 16 Hz, 1H) 3.83 (s, 3H), 4.10−4.14 (m+AB d, J = 16 Hz, 2H), 4.61 (br m, 1H), 6.00 (dd, J_1= 10.0 Hz, J_2= 4.8 Hz, 1H), 6.09 (d, J = 10.0 Hz, 1H), 6.61 (d, J = 8.4 Hz, 1H), 6.66 (d, J = 8.4 Hz, 1H). ^{13}C NMR ($CDCl_3$, 100 MHz) δ 24.36, 27.20, 27.38, 27.51, 28.63, 29.94, 30.14, 30.38, 32.48, 32.91, 33.64, 36.45, 41.26, 42.07, 42.67, 44.02, 47.15, 48.41, 49.69, 50.60, 51.48, 55.88, 55.94, 57.78, 62.07, 88.71, 111.13, 121.99, 126.98, 127.52, 129.52, 133.14, 144.01, 145.76. $[\alpha]^{25}_D$ = −45.8 (c 0.11, $CHCl_3$). UPLC/MS: purity 95%, MS (ESI+): m/z 549.5 $[M + H]^+$.

*(4aS,6R,8aS)-11-(7-((3,5-Dimethyladamantan-1-yl)-(methyl)amino)heptyl)-3-methoxy-5,6,9,10,11,12-hexahydro-4aH-benzo[2,3]benzofuro[4,3-cd]azepin-6-ol (**10**).* **10** was synthesized from **22** (0.190 g, 0.62 mmol). Elution with CH_2Cl_2/CH_3OH/33% aqueous ammonia (9:1:0.15) afforded **10** as a waxy solid: 0.084 g (49%). ^{1}H NMR ($CDCl_3$, 400 MHz) δ 0.82 (s, 6H), 1.03−1.08 (AB m, 2H), 1.22−1.36 (m, 14H), 1.40−1.49 (m, 5H), 1.52−1.55 (m, 2H), 1.95−2.00 (m, 2H), 2.12−2.18 (m, 1H), 2.25 (s, 3H), 2.37−2.48 (m, 4H), 2.67−2.67 (m, 1H), 3.11−3.15 (m, 1H), 3.28−3.31 (m, 1H), 3.78 (AB d, J = 16 Hz, 1H) 3.83 (s, 3H), 4.07−4.11 (m+AB d, J = 16 Hz, 2H), 4.57 (br m, 1H), 5.97 (dd, J_1= 10.0 Hz, J_2= 4.8 Hz, 1H), 6.09 (d, J = 9.6 Hz, 1H), 6.61 (d, J = 8.4 Hz, 1H), 6.66 (d, J = 8.4 Hz, 1H). ^{13} C NMR ($CDCl_3$, 100 MHz) δ 27.32, 27.54, 29.49, 29.65, 29.94, 30.18, 30.50, 32.33, 32.93, 33.73, 36.69, 42.88, 44.33, 48.40, 49.64, 50.79, 51.48, 55.86, 57.76, 62.07, 88.71, 111.11, 121.97, 126.99, 127.51, 129.53, 133.15, 144.00, 145.75. $[\alpha]^{25}_D$ = −50.4 (c 0.11, $CHCl_3$). UPLC/MS: purity 98%, MS (ESI+): m/z 563.5 $[M + H]^+$.

*(4aS,6R,8aS)-11-(8-((3,5-Dimethyladamantan-1-yl)-(methyl)amino)octyl)-3-methoxy-5,6,9,10,11,12-hexahydro-4aH-benzo[2,3]benzofuro[4,3-cd]azepin-6-ol (**11**).* **11** was synthesized from **23** (0.160 g, 0.50 mmol). Elution with CH_2Cl_2/CH_3OH/33% aqueous ammonia (9:1:0.15) afforded **11** as a waxy solid: 0.075 g (52%). ^{1}H NMR ($CDCl_3$, 400 MHz) δ 0.81 (s, 6H), 1.01−1.13 (AB m, 2H), 1.25−1.31 (m, 16H), 1.38−1.46 (m, 5H), 1.47−1.50 (m, 2H), 1.94−2.02 (m, 2H), 2.10−2.11 (m, 1H), 2.19 (s, 3H), 2.31−2.38 (m, 4H), 2.40−2.77 (m, 1H), 3.11−3.15 (m, 1H), 3.28−3.32 (m, 1H), 3.78 (AB d, J = 16 Hz, 1H) 3.83 (s, 3H), 4.07−4.11 (m+AB d, J = 16 Hz, 2H), 4.58 (br m, 1H), 5.97 (dd, J_1= 10.0 Hz, J_2= 5.2 Hz, 1H), 6.07 (d, J = 10.0 Hz, 1H), 6.58 (d, J = 8.4 Hz, 1H), 6.63 (d, J = 8.4 Hz, 1H). ^{13} C NMR ($CDCl_3$, 100 MHz) δ 27.45, 29.54, 29.95, 30.24, 30.62, 32.23, 32.98, 33.90, 37.02, 43.08, 44.74, 48.41, 49.70, 50.99, 51.51, 55.87, 57.81, 62.08. $[\alpha]^{25}_D$ = −48.6 (c 0.11, $CHCl_3$). UPLC/MS: purity 95%, MS (ESI+): m/z 577.5 $[M + H]^+$.

*General Procedure for the Synthesis of **51**−**53**.* To a vigorously stirred solution of **2** hydrochloride (0.300 g, 1.40 mmol) and K_2CO_3 (0.480 g, 3.50 mmol) in MeCN was added dropwise the appropriate acylating agent. The reaction was stirred at room temperature for 4 h. After evaporation of the solvent, the crude was purified by flash chromatography (see Supporting Information for details).

*General Procedure for the Synthesis of **16**−**18**.* A mixture of the chloride derivative (1.2 equiv), **20** (1 equiv), Et_3N (2 equiv), and KI (catalytic amount) in MeCN (0.1 M) was stirred at 80 °C for 48 h in a pressure tube. After evaporation of the solvent, the residue was purified by flash chromatography.

*N-(3,5-Dimethyladamantan-1-yl)-4-((4aS,6R,8aS)-6-hydroxy-3-methoxy-5,6,9,10-tetrahydro-4aH-benzo[2,3]-benzofuro[4,3-cd]azepin-11(12H)-yl)butanamide (**16**).* **16** was synthesized from **51** (0.070 g, 0.25 mmol). Elution with CH_2Cl_2/CH_3OH/33% aqueous ammonia (9:1:0.02) afforded **16** as a waxy solid: 0.070 g (65%). ^{1}H NMR ($CDCl_3$, 400 MHz) δ 0.83 (s, 6H), 1.13−1.15 (AB m, 2H), 1.26−1.38 (AB m, 4H), 1.61 (br m, 4H), 1.72−1.79 (m, 4H), 1.98−2.04 (m, 2H), 2.11−2.14 (m, 3H), 2.47−2.55 (m, 3H), 2.65−2.70 (m, 1H), 3.11−3.18 (m, 1H), 3.31−3.38 (m, 1H), 3.77 (AB d, J = 16 Hz, 1H) 3.83 (s, 3H), 4.09−4.14 (m+AB d, J = 16 Hz, 2H), 4.60 (br m, 1H), 5.57 (br s,1H), 6.00 (dd, J_1= 10.0 Hz, J_2= 4.8 Hz, 1H), 6.09 (d, J = 10.0 Hz, 1H), 6.61 (d, J = 8.4 Hz, 1H), 6.66 (d, J = 8.4 Hz, 1H). ^{13}C NMR ($CDCl_3$, 100 MHz) δ 22.92, 30.05, 32.30, 33.04, 35.24, 40.17, 42.63, 47.60, 48.33, 50.56, 51.52, 53.25, 58.81, 55.89, 55.96, 57.60, 61.98, 88.68, 111.24, 122.04, 126.82, 127.65, 129.01, 133.10, 144.11, 145.82, 172.01. $[\alpha]^{25}_D$ = −60.1 (c 0.11, $CHCl_3$). UPLC/MS: purity 96%, MS (ESI+): m/z 521.4 $[M + H]^+$.

*N-(3,5-Dimethyladamantan-1-yl)-5-((4aS,6R,8aS)-6-hydroxy-3-methoxy-5,6,9,10-tetrahydro-4aH-benzo[2,3]-benzofuro[4,3-cd]azepin-11(12H)-yl)pentanamide (**17**).* **17** was synthesized from **52** (0.070 g, 0.24 mmol). Elution with CH_2Cl_2/CH_3OH/33% aqueous ammonia (9:1:0.02) afforded **17** as a waxy solid: 0.070 g (67%). ^{1}H NMR ($CDCl_3$, 400 MHz) δ 0.83 (s, 6H), 1.11−1.19 (AB m, 2H), 1.24−1.47 (AB m, 4H), (m, 4H), 1.49−1.60 (m, 5H), 1.62−1.80 (br m, 2H), 1.98−2.09 (m, 2H), 2.11−2.14 (m, 3H), 2.44−2.54 (m, 2H), 2.65−2.70 (m, 1H), 3.13−3.17 (m, 1H), 3.31−3.37 (m, 1H), (AB d, J = 15.6 Hz, 1H) 3.83 (s, 3H), 4.09−4.14 (m+AB d, J = 15.6 Hz, 2H), 4.60 (br m, 1H), 5.12 (br s, 1H), 6.00 (dd, J_1= 9.6 Hz, J_2= 5.2 Hz, 1H), 6.08 (d, J = 10.0 Hz, 1H), 6.60 (d, J = 8.0 Hz, 1H), 6.65 (d, J = 8.4 Hz, 1H). ^{13}C NMR ($CDCl_3$, 100 MHz) δ 23.51, 26.87, 30.12, 32.34, 32.99, 37.50, 40.21, 42.63, 47.65, 48.38, 50.57, 51.60, 53.34, 55.92, 57.67, 62.05, 88.72, 111.18, 121.96, 126.94, 127.57, 129.38, 133.15, 144.07, 145.81, 171.97. $[\alpha]^{25}_D$ = −57.8 (c 0.11, $CHCl_3$). UPLC/MS: purity 100%, MS (ESI+): m/z 535.4 $[M + H]^+$.

*N-(3,5-Dimethyladamantan-1-yl)-6-((4aS,6R,8aS)-6-hydroxy-3-methoxy-5,6,9,10-tetrahydro-4aH-benzo[2,3]-benzofuro[4,3-cd]azepin-11(12H)-yl)hexanamide (**18**).* **18** was synthesized from **53** (0.070 g, 0.224 mmol). Elution with CH_2Cl_2/CH_3OH/33% aqueous ammonia (9:1:0.02) afforded **18** as a waxy solid: 0.080 g (78%). ^{1}H NMR ($CDCl_3$, 400 MHz) δ 0.83 (s, 6H), 1.07−1.14 (AB m, 2H), 1.18−1.38 (AB m, 4H), 1.48−1.66 (m, 10H), 1.81 (br m, 2H), 1.96−2.06 (m, 4H), 2.12 br (m, 1H), 2.41−2.54 (m, 3H), 2.41−2.54 (m, 1H), 3.14−3.18 (m, 1H), 3.27−3.37 (m, 1H), 3.77 (AB d, J = 16 Hz, 1H) 3.83 (s, 3H), 4.09−4.14 (m+AB d, J = 16 Hz, 2H), 4.60 (br m, 1H), 5.23 (br s, 1H), 6.00 (dd, J_1= 10.0 Hz, J_2= 4.8 Hz, 1H), 6.09 (d, J = 10.0 Hz, 1H), 6.61 (d, J = 8.4 Hz, 1H), 6.66 (d, J = 8.4 Hz, 1H). ^{13}C NMR ($CDCl_3$, 100 MHz) δ 25.54, 26.84, 27.08, 29.63, 30.04, 32.30, 32.85, 37.52, 40.15, 42.62, 47.58, 48.35, 50.55, 51.43, 53.30, 55.81, 55.87, 57.65, 62.01,

dx.doi.org/10.1021/jm3009458 | J. Med. Chem. XXXX, XXX, XXX−XXX

61.99, 88.67, 111.18, 121.98, 126.91, 127.53, 129.25, 133.09, 144.01, 145.74, 172.17. $[\alpha]^{25}_{D}$ = −60.8 (*c* 0.11, $CHCl_3$). UPLC/MS: purity 100%, MS (ESI+): *m*/*z* 549.5 $[M + H]^+$.

*3-((tert-Butoxycarbonyl)amino)propyl 4-Methylbenzenesulfonate (**69**).* **69** was synthesized starting from 3-aminopropanol according to a literature procedure.[38] ^{1}H NMR ($CDCl_3$, 400 MHz) δ 1.35 (s, 9H), 1.75−1.81 (m, 2H), 2.38, (s, 3H), 3.09 (br m, 2H), 4.02 (t, *J* = 6.0 Hz, 2H), 4.70 (br m, 1H), 7.30 (d, *J* = 8.0 Hz, 2H), 7.72 (d, *J* = 8.0 Hz, 2H).

*tert-Butyl (3-((4aS,6R,8aS)-6-Hydroxy-3-methoxy-5,6,9,10-tetrahydro-4aH-benzo[2,3]benzofuro[4,3-cd]azepin-11-(12H)-yl)propyl)carbamate (**70**).* In a pressure tube a mixture of **69** (0.101 g, 0.31 mmol), **20** (0.070 mg, 0.26 mmol), and Et_3N (0.07 mL, 0.73 mmol) in CH_3CN (3 mL) was stirred at 80 °C for 48 h. After evaporation of the solvent, the residue was purified by flash chromatography. Elution with CH_2Cl_2/CH_3OH (9:1) afforded **70** as a waxy solid: 0.080 g (73%). ^{1}H NMR ($CDCl_3$, 400 MHz) δ 1.40 (s, 9H), 1.47−1.50 (AB m, 1H), 1.55−1.65 (m, 2H), 1.94−2.04 (m, 2H), 2.46−2.56 (m, 2H), 2.63−2.68 (AB m, 1H), 3.11−3.14 (m, 3H), 3.28−3.35 (m, 1H), (AB d, *J* = 15.2 Hz, 1H), 3.81 (s, 3H), 4.07−4.11 (m +AB d, *J* = 15.2 Hz, 2H), 4.57 (br m, 1H), 4.99 (br m, 1H), 5.97 (dd, J_1 = 10.2 Hz, J_2 = 4.3 Hz, 1H), 6.06 (d, *J* = 10.4 Hz, 1H), 6.57 (d, *J* = 8.4, 1H), 6.62 (d, *J* = 8.0, 1H).

*(4aS,6R,8aS)-11-(3-Aminopropyl)-3-methoxy-5,6,9,10,11,12-hexahydro-4aH-benzo[2,3]benzofuro[4,3-cd]-azepin-6-ol (**71**).* HCl (4 M) in dioxane (1 mL) was carefully added to **70** (0.080 g, 0.186 mmol) at 0 °C, and the solution was stirred at room temperature for 2 h. After removal of the solvent, the obtained residue was purified by flash chromatography. Elution with CH_2Cl_2/CH_3OH/33% aqueous ammonia (9:1:0.15) afforded **71** as a waxy solid: 0.046 g (75%). ^{1}H NMR ($CDCl_3$, 400 MHz) δ 1.47−1.50 (AB m, 1H), 1.61−1.72 (m, 2H), 1.94−2.04 (m, 2H), 2.52−2.60 (m, 2H), 2.62−2.66 (AB m, 1H), 2.82 (br m, 2H), 3.14−3.36 (m+br m exchangeable with D_2O, 4H), 3.80 (s, 3H), 3.81 (AB d, *J* = 15.2 Hz, 1H), 4.07−4.11 (m+AB d, *J* = 15.2 Hz, 2H), 4.56 (br m, 1H), 5.96 (dd, J_1 = 10.2 Hz, J_2 = 4.3 Hz, 1H), 6.06 (d, *J* = 10.4 Hz, 1H), 6.58 (d, *J* = 8.4, 1H), 6.60 (d, *J* = 8.0, 1H).

*tert-Butyl (3,5-Dimethyladamantan-1-yl)(3-((3-((4aS,6R,8aS)-6-hydroxy-3-methoxy-5,6,9,10-tetrahydro-4aH-benzo[2,3]benzofuro[4,3-cd]azepin-11(12H)-yl)propyl)-amino)propyl)carbamate (**72**).* In a pressure tube a mixture of **71** (0.046 g, 0.139 mmol), **38** (0.068 mg, 0.14 mmol), and Et_3N (0.039 mL, 0.278 mmol) in MeCN (2 mL) was stirred at 80 °C for 24 h. Elution with CH_2Cl_2/CH_3OH/33% aqueous ammonia (9:1:0.04) afforded **72** as a waxy solid: 0.035 g (39%). ^{1}H NMR ($CDCl_3$, 400 MHz) δ 0.82 (s, 6H), 1.10−1.12 (AB m, 2H), 1.23−1.27 (m, 12H), 1.47 (s, 9H), 1.61−1.68 (m, 4H), 1.79−1.83 (m, 2H), 1.89−2.04 (m, 2H), 2.16 (br m, 1H), 2.53−2.54 (m, 1H), 2.80−2.83 (m, 2H), 2.92−2.94 (m, 1H), 3.03−3.09 (m, 2H), 3.28−3.49 (m, 3H), 3.81 (s, 3H), 3.99 (AB d, *J* = 15.2 Hz, 1H), 4.15 (AB d, *J* = 15.2 Hz, 1H), 4.58 (br m, 1H), 5.98−5.99 (m, 2H), 6.60 (d, *J* = 8.4, 1H), 6.63 (d, *J* = 8.0, 1H).

*(4aS,6R,8aS)-11-(3-((3-((3,5-Dimethyladamantan-1-yl)-amino)propyl)amino)propyl)-3-methoxy-5,6,9,10,11,12-hexahydro-4aH-benzo[2,3]benzofuro[4,3-cd]azepin-6-ol (**15**).* HCl (4 M) in dioxane (1 mL) was carefully added to **72** (0.035 g, 0.05 mmol) at 0 °C, and the solution was stirred at room temperature for 2 h. After removal of the solvent, the obtained residue was purified by flash chromatography. Elution with CH_2Cl_2/CH_3OH/33% aqueous ammonia (9:1:0.20) afforded **15** as a waxy solid: 0.012 g (41%). ^{1}H NMR ($CDCl_3$, 400 MHz) δ 0.84 (s, 6H), 1.09−1.17 (AB m, 2H), 1.17−1.39 (m, 8H), 1.48−1.57 (m, 4H), 1.67−1.68 (m, 2H), 1.79−1.80 (m, 2H), 1.97−2.08 (m, 2H), 2.16 (br m, 1H), 2.49−2.58 (m, 2H), 2.66 (t, *J* = 7.2 Hz, 2H), 2.76−2.83 (m, 4H), 2.90 (br m, exchangeable with D_2O, 1H), 3.13−3−16 (m, 1H), 3.31−3.34 (m, 1H), 3.77−3.81 (s+AB d, *J* = 15.2 Hz, 4H), 4.09−4.13 (m+AB d, *J* = 15.2 Hz, 2H), 4.58 (br m, 1H), 5.97 (dd, J_1 = 10.2 Hz, J_2 = 4.3 Hz, 1H), 6.05 (d, *J* = 10.4 Hz, 1H), 6.60 (d, *J* = 8.4, 1H), 6.63 (d, *J* = 8.0, 1H). ^{13} C NMR ($CDCl_3$, 100 MHz) δ 22.66, 26.86, 29.33, 29.63, 29.67, 29.92, 29.96, 30.07, 31.90, 32.42, 32.93, 39.79, 40.33, 42.58, 47.32, 47.83, 48.40, 49.35, 50.54, 51.76, 55.88, 57.51, 62.03, 88.71, 111.17, 122.02, 126.81, 127.66, 129.13, 133.13, 144.14, 115.82. $[\alpha]^{25}_{D}$ = −40.3 (*c* 0.09, $CHCl_3$). UPLC/MS: purity 95%, MS (ESI+): *m*/*z* 550 $[M + H]^+$.

Biological Evaluation. *Materials.* $[^3H]$Ifenprodil (40 Ci/mmol) and $[^3H]$MK-801 (27.5 Ci/mmol) were obtained from Perkin-Elmer Life Science Inc. (Boston, MA). Memantine and galantamine were obtained from Tocris (Bristol, U.K.). Other compounds and reagents were purchased from Sigma-Aldrich (Milan, Italy).

$[^3H]$MK-801 Binding Assay. Crude synaptic membranes were prepared from the cerebral cortex of Sprague−Dawley rats using a modified method from Marvizòn et al.[39] The cerebral cortex was removed and homogenized in 10 vol. (v/w) of ice-cold 0.32 M sucrose solution. The homogenate was centrifuged at 1000*g* for 10 min and the resulting supernatant centrifuged at 10 000*g* for 20 min. The pellets were washed (resuspended, homogenized, and centrifuged at 48 000*g* for 20 min) twice in 50 vol of Tris−HEPES buffer (Tris 4.5 mM, HEPES 5 mM, pH 7.4) containing EDTA 1 mM and twice in Tris−HEPES buffer without EDTA. The pellets were stored at −80 °C for at least 18 h.

Before the binding assay, the membrane pellets were washed three more times with Tris−HEPES buffer (Tris 4.5 mM, HEPES 5 mM, pH 7.4) to remove the endogenous amino acids. In the binding assay, $[^3H]$MK-801 (final concentration 3 nM), 50 μL of membrane preparation (40−50 μg protein), and 10 μL of compound were mixed at 25 °C in the presence of L-glutamate (10 μM), glycine 50 μL (10 μM). Tris−HEPES buffer (Tris 4.5, HEPES 5 mM, pH 7.4) was added to a final volume of 0.5 mL. Following incubation for 2 h at 25 °C, binding was terminated by filtration using Whatman GF/B filters and a Brandel M-48 Cell Harvester. Radioactivity was measured using a PerkinElmer liquid scintillation counter. Nonspecific binding was determined in the presence of unlabeled 100 μM (1)-MK-801. The dissociation constant (K_d) of $[^3H]$MK-801 in rat cortex membranes was 4.0 nM. For compound activity determination, aliquots of membrane pellets were incubated with different ligand concentrations in the presence of 3 nM $[^3H]$MK-801 for 2 h at 25 °C. Samples were then filtered, and the radioactivity was counted.

$[^3H]$Ifenprodil Binding Assay. Rat cortex membranes were prepared as previously reported.[40] The frontal cortex membranes from adult male Sprague−Dawley rats were pooled and homogenized in 10 volumes of ice-cold 0.32 M sucrose/50 mM Tris/acetate buffer (pH 7.4) (homogenizing buffer) in a Teflon pestle homogenizer. The homogenate was centrifuged at 1000*g* for 10 min at 4 °C, and the supernatant was collected. The pellet was dissolved in a small volume of homogenizing buffer and centrifuged again at 1000*g* for 10 min at 4 °C. The supernatant was collected together with the first supernatant

dx.doi.org/10.1021/jm3009458 | J. Med. Chem. XXXX, XXX, XXX−XXX

and centrifuged at 17 000*g* for 20 min at 4 °C. The pellet (P2) was homogenized in 20 volumes of ice-cold 50 mM Tris/acetate buffer, pH 7.0 and centrifuged at 50 000*g* for 30 min at 4 °C. This last centrifugation step was repeated three times. The final pellet was suspended in ice-cold 50 mM Tris/acetate buffer, pH 7.0, and aliquots of 0.5 mL were stored at −80 °C. The protein content was measured by the method described by Lowry et al.[41]

The assay was carried out in a total volume of 500 μL, in the presence of about 10 nM [^{3}H]ifenprodil in binding buffer containing 50 μg of protein and 100 μM of trifluoperazine, to block the non-NMDA receptor [^{3}H]ifenprodil binding. Unlabeled ifenprodil, 100 μM, was used to define nonspecific binding. After 2 h of incubation at 25 °C in a water bath, bound radioligand was separated from unbound by filtration through presoaked (0.5% polyethyleneimine solution) presoaked glass fiber filters (Whatman GF/B) under reduced pressure. The filters were rinsed with 4 mL of cold binding buffer three times. The filters were placed into individual 4 mL scintillation vials and prepared for counting using conventional liquid spectroscopy. The radioactivity was measured in a β-counter. The dissociation constant (K_d) of [^{3}H]ifenprodil in rat cortex membranes was 28.0 nM. All compounds were routinely dissolved in DMSO and diluted with assay buffer to the final concentration with the final amount of DMSO never exceeding 2%. Percent inhibition values for specific radiolabeled ligand binding results at 10−100 μM concentration are means ± SEM of at least three determinations. At least five different concentrations (spanning 3 orders of magnitude) were adjusted appropriately for the IC_{50} of each compound examined. IC_{50} values were computer-generated using a nonlinear regression formula (Graph-Pad, San Diego, CA) and were converted to K_i values using the known K_d values of the radioligands in the different tissues and using the Cheng−Prusoff equation.[42] K_i values were means ± SEM of at least three determinations.

Rat Acetylcholinesterase (AChE) Inhibition Assays. The cholinesterase assay method of Ellman[25] was used to determine the in vitro cholinesterase activity. The activity was measured by increase in absorbance at 412 nm due to the yellow color produced from the reaction of acetylthiocholine iodide with the dithiobisnitrobenzoate (DTNB) ion. AChE was prepared from the brain of Wistar rats by homogenizing under a Teflon blender for 10 min in 0.1 M KH_2PO buffer, pH 8. A stock solution of the enzyme in 0.1 M KH_2PO buffer (pH 8), containing 0.1% Triton X-100, was kept frozen. Acetylthiocholine iodide and DTNB were prepared daily using 0.1 M KH_2PO_4 buffer (pH 7). The assay solution consisted of a 0.1 M phosphate buffer, pH 8.0, with the addition of 340 μM DTNB, 0.02 unit/mL of rat AChE, and 550 μM of substrate (acetylthiocholine iodide).

Assay solutions were preincubated for 10 min at 37 °C, followed by the addition of substrate. The inhibitory activity of the newly synthesized compounds was assayed by adding different compound concentrations to the reaction mixture described above. All the inhibitors were dissolved in DMSO, whose concentration never exceeded 1% in the final reaction mixture. The rate of the increase in absorbance at 412 nm was followed for 5 min at 37 °C with a PerkinElmer spectrophotometer. Assays were carried out with a blank containing all components except AChE to account for the nonenzymatic reaction. The reaction rates were compared, and the percent inhibition due to the presence of tested compounds was calculated. Data are expressed as percentage of inhibition ± SEM of AChE activity, set to 100%. IC_{50} values were determined graphically from log concentration−inhibition curves (GraphPad Prism 4.03 software, GraphPad Software Inc.).

Cell Culture, Pharmacological Treatments, and Viability Assay. SHSY-5Y cells were maintained in DMEM/F12 medium supplemented with 15% fetal bovine serum, 1% nonessential amino acids, 2 mM L-glutamine, and penicillin/streptomycin in a humidified atmosphere (5% CO_2) at 37 °C.

Cells were seeded in 96-well microplates (5000 cells/well); on the next day, cells were incubated with 500 μM NMDA, in the absence or presence of different compound concentrations. At least six different concentrations, ranging from 0.01 nM to 100 μM, were tested for standard and newly synthesized compounds. The compounds were added for 5 min prior to addition of NMDA, to determine the inhibition of NMDA-mediated cell toxicity.

Following incubation times, cell viability was determined using the MTS assay according to the manufacturer's instructions. The dehydrogenase activity in active mitochondria reduced 3-(4,5-dimethylthiazol-2-yl)-5-(3-carboxymethoxyphenyl)-2-(4-sulfophenyl)-2*H*-tetrazolium (MTS) to the soluble formazan product. The absorbance of formazan at 490 nM was measured in a colorimetric assay with an automated plate reader.

Within an experiment, each condition was assayed in duplicate or triplicate and each experiment was performed at least three times. The results were calculated by subtracting the mean background from the values obtained from each test condition and were expressed as the percentage of the control (untreated cells). A nonlinear multipurpose curve-fitting program, Prism (GraphPad Software Inc., San Diego, CA), was used for data analysis of cell viability; the IC_{50} value represents the compound concentration able to give 50% of NMDA-induced toxicity. Student's *t* test was used to evaluate whether differences between the experimental groups and the control were statistically significant.

Docking Simulations. Ligand docking simulations were performed on a receptor model generated using ICM3.7[43] based on the crystal structure of the human AChE solved in complex with fasciculin (PDB code: 1B41).[44] Fasciculin was removed from the complex. The protein atoms were assigned the correct atom types according to a modified version of the ECEPP/3 force field. Hydrogen atoms were added. Heavy side chain atoms that were not solved in the crystal structure and assigned occupancy equal to zero (Glu268: cg, cd, oe1, oe2; Gln291: cd, oe1, ne2; Gln369: cd, oe1, ne2; Arg522: cz, nh1, nh2) were added according to the topology of the ICM library of standard residues. None of these side chain atoms turned out to be involved in the definition of the binding pocket (see below), being either far from the binding site or pointing toward the bulk of the solvent.

The side chains of the residues lining the enzyme gorge had to be optimized to allow relaxing of the conformation of Tyr337 and nearby residues in such a way as to bind bulky ligands. For this purpose, the structure of the human enzyme was superimposed and tethered to the crystal structure of TcAChE solved in complex with a dual derivative of **1** (PDB code 1W4L)[21] using the ICM built-in impose_conformation macro. It appeared safe to adopt this procedure because of the high level of conservation between the two orthologues. According to BLAST, TcAChE and hAChE shared 58.9% sequence identity[45] and 75% homology.[46] The superimposition

dx.doi.org/10.1021/jm3009458 | J. Med. Chem. XXXX, XXX, XXX−XXX

procedure was based on an iterative algorithm[47] that attempts to find the ideal overlapping core between structures. Atom equivalences were established on the fly according to sequence alignment. On account of this approach, a minority of deviating atoms did not affect the overall quality of the superimposition. Then, the tethering procedure pulled hAChE atoms toward the positions of corresponding atoms in TcAChE according to the alignment and by means of harmonic restraints. Finally, tautomeric states of histidines, the positions of asparagine and glutamine side-chain amidic groups, and the side chains in which heavy atoms were added were optimized through a Monte Carlo procedure to improve the hydrogen bonding pattern in the new conformation. Polar hydrogen atoms were also optimized. Ligands were assigned the MMFF force field atom types and charges.[48]

The boundaries of the binding pocket were defined by selecting all the residues with at least one side-chain non-hydrogen atom in the range of 5 Å from the crystallographic position of a previously reported dual derivative of **1** (PDB code 1W4L).[21] When considering only the binding site residues, sequence identity between hAChE and TcAChE was 86% and homology 94%. The backbone displacement in the generated hAChE binding pocket conformation measured in terms of RMSD with respect to the original crystal structure was 0.7 Å (1.0 Å including side-chain heavy atoms). Tyr337 was the only amino acid that displayed a significant conformational rearrangement. As expected, the dihedral angles describing the position of the Tyr337 side chain in hAChE ($\chi1$ −133, $\chi2$ −34) ended up closely resembling those of Phe330 in TcAChE ($\chi1$ −137, $\chi2$ −39).

Docking simulations were carried out by means of the Biased Probability Monte Carlo stochastic optimizer as implemented in ICM. The molecular conformation of the system was described by means of internal coordinate variables. The binding site residues were described by precalculated 0.5 Å spacing potential grid maps, representing van der Waals potentials for hydrogens and heavy atoms, electrostatics, hydrophobicity, and hydrogen bonding, respectively. The van der Waals interactions were described by a smoother form of the 6−12 Lennard−Jones potential with the repulsive contribution capped at a cutoff value of 4 kcal/mol. Poses from Monte Carlo sampling were rescored by means of the standard ICM empirical scoring function.

5 was docked into the crystal structure of the heterodimer formed by the amino terminal domains of N1 and N2B subunits of NMDA receptor solved in complex with ifenprodil.[49] The simulation was performed according to the SCARE induced fit docking protocol that has been thoroughly described by Bottegoni and colleagues,[50] and it is only briefly summarized here. SCARE implements the flexibility of the receptor in the simulation generating different local versions of the binding pocket. The protein atoms were assigned the correct atom types according to a modified version of the ECEPP/3 force field. Hydrogen atoms were added. Tautomeric states of histidines, the positions of asparagine and glutamine side-chain amidic groups, and polar hydrogen atoms were optimized. The binding pocket boundaries were defined, selecting the residues with at least one non-hydrogen atom within 5 Å from the crystallographic position of ifenprodil. Then, ifenprodil was removed from the structure. **5** was assigned the MMFF force field atom types and charges.[48] Twelve variants of the receptor binding pocket were generated, systematically omitting pairs of proximal side chains. **5** was docked at each variant according to the already described ICM standard Monte Carlo docking protocol (see above). The best scoring poses were collected and employed to seed independent optimization runs on the receptor, after restoring the original pocket composition and conformation. For each optimized complex, the binding score was calculated. The complex returning the best score was proposed as the putative binding mode.

■ ASSOCIATED CONTENT

Ⓢ Supporting Information

Docking models of AChE in complex with **5**, **7**, **8**, and **12**−**18**. Docking model of NR2B-containing NMDAR in complex with **5**. Effect of galantamine on NMDA-induced toxicity in SHSY-5Y cells. Experimental details of chemical syntheses of intermediates **21**−**68**. This material is available free of charge via the Internet at http://pubs.acs.org.

■ AUTHOR INFORMATION

Corresponding Author

*(A.C.) E-mail: andrea.cavalli@iit.it, phone/fax: +39 010 71781530/710187; (M.R.) e-mail: michela.rosini@unibo.it, phone/fax: +39 051 2099722/34.

Notes

The authors declare the following competing financial interest(s): A patent protecting the class of compounds disclosed in this paper was filed by the following authors: Cavalli, A.; Rosini, M.; Simoni, E.; Reggiani, A.; Melchiorre, C.

■ ACKNOWLEDGMENTS

We thank Sine Mandrup Bertozzi for technical assistance. We thank Grace Fox for editing and proofreading the manuscript. Tiziano Bandiera is gratefully acknowledged for useful discussions. C.M. and M.R. gratefully acknowledge MIUR for the financial support (PRIN 2009ESXPT2_001).

■ ABBREVIATIONS USED

AChE, acetylcholinesterase; AD, Alzheimer's disease; DTNB, dithiobisnitrobenzoate; LELP, ligand efficiency lipophilicity; MTDLs, multitarget-directed ligands; MTS, 3-(4,5-dimethylthiazol-2-yl)-5-(3-carboxymethoxyphenyl)-2-(4-sulfophenyl)-2*H*-tetrazolium; NMDA, *N*-methyl-D-aspartate; NMDAR, *N*-methyl-D-aspartate receptor; NR2B, 2B subunit of the NMDA receptor

■ REFERENCES

(1) Alzheimer's Disease International, World Alzheimer Report. http://www.alz.co.uk/research/files/WorldAlzheimerReport2010ExecutiveSummary.pdf

(2) Citron, M. Alzheimer's disease: strategies for disease modification. *Nat. Rev. Drug Discovery* **2010**, *9*, 387−398.

(3) Nordberg, A. Neuroreceptor changes in Alzheimer disease. *Cerebrovasc. Brain Metab. Rev.* **1992**, *4*, 303−328.

(4) Palmer, A. M.; Gershon, S. Is the neuronal basis of Alzheimer's disease cholinergic or glutamatergic? *FASEB J.* **1990**, *4*, 2745−2752.

(5) Schmitt, B.; Bernhardt, T.; Moeller, H. J.; Heuser, I.; Frolich, L. Combination therapy in Alzheimer's disease: a review of current evidence. *CNS Drugs* **2004**, *18*, 827−844.

(6) Patel, L.; Grossberg, G. T. Combination therapy for Alzheimer's disease. *Drugs Aging* **2011**, *28*, 539−546.

(7) Hardingham, G. E.; Bading, H. Synaptic versus extrasynaptic NMDA receptor signalling: implications for neurodegenerative disorders. *Nat. Rev. Neurosci.* **2010**, *11*, 682−696.

(8) Xia, P.; Chen, H. S.; Zhang, D.; Lipton, S. A. Memantine preferentially blocks extrasynaptic over synaptic NMDA receptor currents in hippocampal autapses. *J. Neurosci.* **2010**, *30*, 11246−11250.
(9) Samochocki, M.; Hoffle, A.; Fehrenbacher, A.; Jostock, R.; Ludwig, J.; Christner, C.; Radina, M.; Zerlin, M.; Ullmer, C.; Pereira, E. F.; Lubbert, H.; Albuquerque, E. X.; Maelicke, A. Galantamine is an allosterically potentiating ligand of neuronal nicotinic but not of muscarinic acetylcholine receptors. *J. Pharmacol. Exp. Ther.* **2003**, *305*, 1024−1036.
(10) Santos, M. D.; Alkondon, M.; Pereira, E. F.; Aracava, Y.; Eisenberg, H. M.; Maelicke, A.; Albuquerque, E. X. The nicotinic allosteric potentiating ligand galantamine facilitates synaptic transmission in the mammalian central nervous system. *Mol. Pharmacol.* **2002**, *61*, 1222−1234.
(11) Moriguchi, S.; Marszalec, W.; Zhao, X.; Yeh, J. Z.; Narahashi, T. Mechanism of action of galantamine on N-methyl-D-aspartate receptors in rat cortical neurons. *J. Pharmacol. Exp. Ther.* **2004**, *310*, 933−942.
(12) McGehee, D. S.; Heath, M. J.; Gelber, S.; Devay, P.; Role, L. W. Nicotine enhancement of fast excitatory synaptic transmission in CNS by presynaptic receptors. *Science* **1995**, *269*, 1692−1696.
(13) Geerts, H.; Grossberg, G. T. Pharmacology of acetylcholinesterase inhibitors and N-methyl-D-aspartate receptors for combination therapy in the treatment of Alzheimer's disease. *J. Clin. Pharmacol.* **2006**, *46*, 8S−16S.
(14) Grossberg, G. T.; Edwards, K. R.; Zhao, Q. Rationale for combination therapy with galantamine and memantine in Alzheimer's disease. *J. Clin. Pharmacol.* **2006**, *46*, 17S−26S.
(15) Cavalli, A.; Bolognesi, M. L.; Minarini, A.; Rosini, M.; Tumiatti, V.; Recanatini, M.; Melchiorre, C. Multi-target-directed ligands to combat neurodegenerative diseases. *J. Med. Chem.* **2008**, *51*, 347−372.
(16) Zimmermann, G. R.; Lehar, J.; Keith, C. T. Multi-target therapeutics: when the whole is greater than the sum of the parts. *Drug Discovery Today* **2007**, *12*, 34−42.
(17) Morphy, R.; Rankovic, Z. Fragments, network biology and designing multiple ligands. *Drug Discovery Today* **2007**, *12*, 156−160.
(18) Hopkins, A. L. Network pharmacology: the next paradigm in drug discovery. *Nat. Chem. Biol.* **2008**, *4*, 682−690.
(19) Small, G.; Dubois, B. A review of compliance to treatment in Alzheimer's disease: potential benefits of a transdermal patch. *Curr. Med. Res. Opin.* **2007**, *23*, 2705−2713.
(20) Bottegoni, G.; Favia, A. D.; Recanatini, M.; Cavalli, A. The role of fragment-based and computational methods in polypharmacology. *Drug Discovery Today* **2012**, *17*, 23−34.
(21) Greenblatt, H. M.; Guillou, C.; Guenard, D.; Argaman, A.; Botti, S.; Badet, B.; Thal, C.; Silman, I.; Sussman, J. L. The complex of a bivalent derivative of galanthamine with torpedo acetylcholinesterase displays drastic deformation of the active-site gorge: implications for structure-based drug design. *J. Am. Chem. Soc.* **2004**, *126*, 15405−15411.
(22) Rosini, M.; Simoni, E.; Bartolini, M.; Cavalli, A.; Ceccarini, L.; Pascu, N.; McClymont, D. W.; Tarozzi, A.; Bolognesi, M. L.; Minarini, A.; Tumiatti, V.; Andrisano, V.; Mellor, I. R.; Melchiorre, C. Inhibition of acetylcholinesterase, β-amyloid aggregation, and NMDA receptors in Alzheimer's disease: a promising direction for the multi-target-directed ligands gold rush. *J. Med. Chem.* **2008**, *51*, 4381−4384.
(23) Rook, Y.; Schmidtke, K. U.; Gaube, F.; Schepmann, D.; Wunsch, B.; Heilmann, J.; Lehmann, J.; Winckler, T. Bivalent β-carbolines as potential multitarget anti-Alzheimer agents. *J. Med. Chem.* **2010**, *53*, 3611−3617.
(24) da Silva, R. A.; Estevam, I. H. S.; Bieber, L. W. Reductive methylation of primary and secondary amines and amino acids by aqueous formaldehyde and zinc. *Tetrahedron Lett.* **2007**, *48*, 7680−7682.
(25) Ellman, G. L.; Courtney, K. D.; Andres, V., jr.; Featherstone, R. M. A new and rapid colorimetric determination of acetylcholinesterase activity. *Biochem. Pharmacol.* **1961**, *7*, 88−90.
(26) Pang, Y. P.; Quiram, P.; Jelacic, T.; Hong, F.; Brimijoin, S. Highly potent, selective, and low cost bis-tetrahydroaminacrine inhibitors of acetylcholinesterase. Steps toward novel drugs for treating Alzheimer's disease. *J. Biol. Chem.* **1996**, *271*, 23646−23649.
(27) Carlier, P. R.; Chow, E. S.; Han, Y.; Liu, J.; El Yazal, J.; Pang, Y. P. Heterodimeric tacrine-based acetylcholinesterase inhibitors: investigating ligand−peripheral site interactions. *J. Med. Chem.* **1999**, *42*, 4225−4231.
(28) Piazzi, L.; Rampa, A.; Bisi, A.; Gobbi, S.; Belluti, F.; Cavalli, A.; Bartolini, M.; Andrisano, V.; Valenti, P.; Recanatini, M. 3-(4-[[Benzyl(methyl)amino]methyl]phenyl)-6,7-dimethoxy-2*H*-2-chromenone (AP2238) inhibits both acetylcholinesterase and acetylcholinesterase-induced β-amyloid aggregation: a dual function lead for Alzheimer's disease therapy. *J. Med. Chem.* **2003**, *46*, 2279−2282.
(29) Belluti, F.; Rampa, A.; Piazzi, L.; Bisi, A.; Gobbi, S.; Bartolini, M.; Andrisano, V.; Cavalli, A.; Recanatini, M.; Valenti, P. Cholinesterase inhibitors: xanthostigmine derivatives blocking the acetylcholinesterase-induced β-amyloid aggregation. *J. Med. Chem.* **2005**, *48*, 4444−4456.
(30) Bolognesi, M. L.; Cavalli, A.; Valgimigli, L.; Bartolini, M.; Rosini, M.; Andrisano, V.; Recanatini, M.; Melchiorre, C. Multi-target-directed drug design strategy: from a dual binding site acetylcholinesterase inhibitor to a trifunctional compound against Alzheimer's disease. *J. Med. Chem.* **2007**, *50*, 6446−6449.
(31) Cavalli, A.; Bolognesi, M. L.; Capsoni, S.; Andrisano, V.; Bartolini, M.; Margotti, E.; Cattaneo, A.; Recanatini, M.; Melchiorre, C. A small molecule targeting the multifactorial nature of Alzheimer's disease. *Angew. Chem., Int. Ed. Engl.* **2007**, *46*, 3689−3692.
(32) Piazzi, L.; Cavalli, A.; Colizzi, F.; Belluti, F.; Bartolini, M.; Mancini, F.; Recanatini, M.; Andrisano, V.; Rampa, A. Multi-target-directed coumarin derivatives: hAChE and BACE1 inhibitors as potential anti-Alzheimer compounds. *Bioorg. Med. Chem. Lett.* **2008**, *18*, 423−426.
(33) Lipton, S. A. Paradigm shift in neuroprotection by NMDA receptor blockade: memantine and beyond. *Nat. Rev. Drug Discovery* **2006**, *5*, 160−170.
(34) Bolognesi, M. L.; Cavalli, A.; Melchiorre, C. Memoquin: a multi-target-directed ligand as an innovative therapeutic opportunity for Alzheimer's disease. *Neurotherapeutics* **2009**, *6*, 152−162.
(35) Mony, L.; Kew, J. N.; Gunthorpe, M. J.; Paoletti, P. Allosteric modulators of NR2B-containing NMDA receptors: molecular mechanisms and therapeutic potential. *Br. J. Pharmacol.* **2009**, *157*, 1301−1317.
(36) Chazot, P. L. The NMDA receptor NR2B subunit: a valid therapeutic target for multiple CNS pathologies. *Curr. Med. Chem.* **2004**, *11*, 389−396.
(37) Liu, Z.; Lv, C.; Zhao, W.; Song, Y.; Pei, D.; Xu, T. NR2B-Containing NMDA Receptors Expression and Their Relationship to Apoptosis in Hippocampus of Alzheimer's Disease-Like Rats. *Neurochem. Res.* **2012**, *37*, 1420−1427.
(38) Nguyen, C.; Ruda, G. F.; Schipani, A.; Kasinathan, G.; Leal, I.; Musso-Buendia, A.; Kaiser, M.; Brun, R.; Ruiz-Perez, L. M.; Sahlberg, B. L.; Johansson, N. G.; Gonzalez-Pacanowska, D.; Gilbert, I. H. Acyclic nucleoside analogues as inhibitors of *Plasmodium falciparum* dUTPase. *J. Med. Chem.* **2006**, *49*, 4183−4195.
(39) Marvizon, J. C.; Lewin, A. H.; Skolnick, P. 1-Amino-cyclopropane carboxylic acid: a potent and selective ligand for the glycine modulatory site of the N-methyl-D-aspartate receptor complex. *J. Neurochem.* **1989**, *52*, 992−994.
(40) Johansson, T.; Frandberg, P. A.; Nyberg, F.; Le Greves, P. Low concentrations of neuroactive steroids alter kinetics of [^{3}H]ifenprodil binding to the NMDA receptor in rat frontal cortex. *Br. J. Pharmacol.* **2005**, *146*, 894−902.
(41) Lowry, O. H.; Rosebrough, N. J.; Farr, A. L.; Randall, R. J. Protein measurement with the Folin phenol reagent. *J. Biol. Chem.* **1951**, *193*, 265−275.
(42) Cheng, Y.; Prusoff, W. H. Relationship between the inhibition constant (K1) and the concentration of inhibitor which causes 50% inhibition (I50) of an enzymatic reaction. *Biochem. Pharmacol.* **1973**, *22*, 3099−3108.

(43) Abagyan, R.; Totrov, M.; Kuznetsov, D. ICM-A new method for protein modeling and design: Applications to docking and structure prediction from the distorted native conformation. *J. Comput. Chem.* **1994**, *15*, 488−506.
(44) Kryger, G.; Harel, M.; Giles, K.; Toker, L.; Velan, B.; Lazar, A.; Kronman, C.; Barak, D.; Ariel, N.; Shafferman, A.; Silman, I.; Sussman, J. L. Structures of recombinant native and E202Q mutant human acetylcholinesterase complexed with the snake-venom toxin fasciculin-II. *Acta Crystallogr., Sect. D: Biol. Crystallogr.* **2000**, *56*, 1385−1394.
(45) Altschul, S. F.; Madden, T. L.; Schaffer, A. A.; Zhang, J.; Zhang, Z.; Miller, W.; Lipman, D. J. Gapped BLAST and PSI-BLAST: a new generation of protein database search programs. *Nucleic Acids Res.* **1997**, *25*, 3389−3402.
(46) Altschul, S. F.; Wootton, J. C.; Gertz, E. M.; Agarwala, R.; Morgulis, A.; Schaffer, A. A.; Yu, Y. K. Protein database searches using compositionally adjusted substitution matrices. *FEBS J.* **2005**, *272*, 5101−5109.
(47) Bottegoni, G.; Kufareva, I.; Totrov, M.; Abagyan, R. Four-dimensional docking: a fast and accurate account of discrete receptor flexibility in ligand docking. *J. Med. Chem.* **2009**, *52*, 397−406.
(48) Halgren, T. A. Merck molecular force field. I−V. *J. Comput. Chem.* **1996**, *17*, 490−641.
(49) Karakas, E.; Simorowski, N.; Furukawa, H. Subunit arrangement and phenylethanolamine binding in GluN1/GluN2B NMDA receptors. *Nature* **2011**, *475*, 249−53.
(50) Bottegoni, G.; Kufareva, I.; Totrov, M.; Abagyan, R. A new method for ligand docking to flexible receptors by dual alanine scanning and refinement (SCARE). *J. Comput.-Aided Mol. Des.* **2008**, *22*, 311−325.